

The Effects of a Stellar Encounter on a Planetesimal Disk

Hiroshi Kobayashi and Shigeru Ida

*Department of Earth and Planetary Sciences,
Tokyo Institute of Technology*

Meguro-ku, Tokyo 152-8551, Japan

hkobayas@geo.titech.ac.jp

ABSTRACT

We investigate the effects of a passing stellar encounter on a planetesimal disk through analytical calculations and numerical simulations, and derive the boundary radius (a_{planet}) outside which planet formation is inhibited by disruptive collisions with high relative velocities. Ida, Larwood, and Burkert (2000, ApJ, 528, 1013-1025) suggested that a stellar encounter caused inhibition of planet formation in the outer part of a protoplanetary disk. We study orbital eccentricity (e) and inclination (i) of planetesimals pumped up by perturbations of a passing single star. We also study the degree of alignment of longitude of pericenter and ascending node to estimate relative velocities between the planetesimals. We model a protoplanetary system as a disk of massless particles circularly orbiting a host star, following Ida *et al.* (2000). The massless particles represent planetesimals. A single star as massive as the host star encounters the protoplanetary system. Numerical orbital simulations show that in the inner region at semimajor axis $a \lesssim 0.2D$ where D is pericenter distance of the encounter, e and i have power-law dependence on (a/D) as $e \propto (a/D)^{5/2}$ and $i \propto (a/D)^{3/2}$ and the longitudes are aligned, independent of the encounter parameters. In the outer region $a \gtrsim 0.2D$, the radial gradient is steeper, and is not expressed by a single power-law. The longitudes are not aligned. Since planet accretion is inhibited by e as small as 0.01, we focus on the weakly perturbed inner region. We analytically reproduce the power-law dependence and explicitly give numerical factors of the power-law dependence as functions of encounter parameters. We derive the boundary radius (a_{planet}) of planet forming region as a function of dynamical parameters of a stellar cluster, assuming the protoplanetary system belongs to the stellar cluster. Since the radial gradient of e is so steep that the boundary is sharply determined. Planetesimal orbits are significantly modified beyond the boundary, while they are almost intact inside the boundary. This tendency is strengthened by reduction of relative velocity due to the longitude alignment in the inner region. We find $a_{\text{planet}} \sim 40\text{-}60\text{AU}$ in the case of $D \sim 150\text{-}200\text{AU}$. $D \sim 200\text{AU}$ may be likely to occur in a relatively dense cluster. We point out that the size of planetary systems (a_{planet}) born in a dense cluster may be necessarily restricted to that comparable to the size of planet region ($\sim 30\text{-}40\text{AU}$) of our Solar system.

Subject headings: celestial mechanics; orbits; planetesimal; accretion

1. INTRODUCTION

In general, stars are born as members of an open cluster. Stellar clusters would evaporate on timescales more than 10^8 years (Kroupa 1995; 1998). This evaporation would be caused by gravitational interactions between stars, so that many stars experience gravitational perturbations of the other stars during the evaporation. More than half of T Tauri stars have protoplanetary disks (e.g., Beckwith and Sargent 1996), which would eventually form planetary systems on timescales 10^6 - 10^9 years (e.g., Safronov 1969; Wetherill 1980; Hayashi *et al.* 1985). Planetary systems would be affected by stellar encounters more or less during their formation stage.

In the standard model (e.g., Safronov 1969; Wetherill 1980; Hayashi *et al.* 1985; Lissauer and Stewart 1993), terrestrial planets and cores of jovian planets accrete from planetesimals that are formed in a protoplanetary disk. The accretion of jovian planet cores is followed by gas accretion onto the core when the core acquires critical mass ~ 5 - $15 M_{\oplus}$ (e.g., Mizuno 1980; Bodenheimer and Pollack 1986; Ikoma *et al.* 2000).

The passing stellar encounters would pump up orbital eccentricity e and inclination i of planetesimals. The velocity dispersion of planetesimals is given by $\sim \sqrt{e^2 + i^2} v_{\text{kep}}$, where i is given in unit of radian and v_{kep} is Keplerian velocity (e.g., Safronov 1969; Lissauer and Stewart 1993; Ohtsuki *et al.* 1993). If the velocity dispersion exceeds their surface escape velocity of planetesimals, a collision between the planetesimals results in disruption rather than accretion because of the high velocity collision unless their pericenters are aligned (e.g., Safronov 1969; Greenberg *et al.* 1978; Ohtsuki 1993; also see section 2). Then, planetesimal accretion would be forestalled. As shown in Eq. (5) in section 2, if pumped-up e and i are larger than 0.01, the velocity dispersion exceeds the surface escape velocity of planetesimals in the early stage. Therefore, small orbital modification ($e, i \gtrsim 0.01$) can give significant influence on planet formation. If the longitudes of pericenter and ascending nodes of colliding planetesimals are aligned (“phase alignment”), the colliding velocity is significantly reduced from that in the above argument (Marzari and Scholl 2000; also see section 6). Hence, we also examine the degree of the alignment.

This work is motivated by Ida, Larwood, and Burkert (2000; hereafter ILB00). They showed that the radial gradient of the pumped-up e and i is rather steep; e and i are highly pumped up in the outer planetesimal disk, while the inner disk is almost intact (also see sections 3 and 4). The steep gradient leads to a sharp boundary of the disk that divides the strongly perturbed region where planet formation is inhibited and the intact region where planet formation keeps going. The boundary radius determines radial size of the region of a planetary system where planetary-sized bodies exist. Most planetesimals in the outermost region are ejected (and some of them are captured by the passing star), which would truncate the region of the planetary system where solid materials exist. Here we are concerned with the former size.

In the present paper, we investigate the orbital modification due to a passing stellar encounter and discuss the effects on planetary formation. We derive analytical formulae of pumped up e and i , because, as stated above, the boundary between the planet forming region and the planet-formation inhibited region is marked by e, i as small as 0.01 and hence linear perturbation analysis is available to determine the boundary. We also did numerical simulations of 10,000 test particles in some parameter ranges. Our analytical formulae show excellent agreement with the numerical results.

Encounters between a star and a particle/gas disk have been studied by many authors in different contexts. However, most previous studies were concerned with the strongly perturbed region in the disk.

Galactic encounters may form galactic tidal bridges and tails. Many numerical simulations (e.g., Toomre and Toomre 1972; Barnes and Hernquist 1992 and references therein) have been done and analytical calculations with impulse approximation was applied for high speed galactic encounters (e.g., Binney and Tremaine 1987). Kalas and Jewitt (1995) suggested that asymmetry in the dust disk around β Pic is caused by a passing stellar encounter. Kalas *et al.* (2000) and Larwood and Kalas (2001) demonstrated through numerical simulation that a passing stellar encounter reproduces the observed disk asymmetry and ringlet structure. These structure in galactic and dust disks is formed in the outer part of a disk which is strongly perturbed.

A galaxy may be captured by another galaxy through energy transfer from orbital motions to internal motions caused by a close encounter to be a satellite galaxy (Palmer and Papaloizou 1982; Wahde *et al.* 1996). Similarly, an encounter of a star with another star with a protoplanetary gas disk may lead to capture of the passing star to form binary stars. It may also make a new companion from the disk (Boffin *et al.* 1998), cause disk truncation (Hall 1997), or cause rapid disk accretion (Ostriker 1994). The transfer of energy and angular momentum between a passing star and the disk is calculated numerically (Clarke and Pringle 1991; Hall *et al.* 1996; Heller 1993; 1995) and analytically (Ostriker 1994). Korycansky and Papaloizou (1995) and Larwood (1997) did more detailed analytical calculations. These studies were mostly concerned with total energy and angular momentum transfer, that is, concerned with strongly perturbed regions in the disk.

Ostriker (1994) also studied weakly perturbed regime, although the author mainly focused on the strongly perturbed region where resonant effects are important. The author only presented approximately averaged change in angular momentum in the weakly perturbed region. As we discuss later, the author’s results would not give enough information to deduce change in e and i , which we want to use to discuss the effects on planet accretion.

Passing stellar encounters are also important for planetary systems or planetesimal disks. The planetesimals ejected by jovian planets may become weakly bounded in the Solar system to form Oort cloud. Passing stellar encounters would make their binding stronger (Brunini and Fernández 1996; Fernández 1997) or send them back to inner Solar system as long-period comets (Eggers and Woolfson 1996; Yabushita *et al.* 1982). They considered stellar encounters with planetesimals

ejected from a protoplanetary system.

At present, mean distance between stars in the solar neighborhood is so large that only Oort cloud would be affected by passing stellar encounters. However, since stars are generally born as members of an open cluster and stay in the cluster on timescales more than 10^8 years (Kroupa 1995; 1998), passing stellar encounters affect a planetary system or a protoplanetary planetesimal system itself in the early stage. Monte-Carlo numerical simulations suggest that the encounters can modify nearly circular orbits of giant planets to eccentric orbits, which may correspond to observed extrasolar planets in eccentric orbits (de la Fuente Marcos and de la Fuente Marcos 1997; Laughlin and Adams 1998; 2000; Bonnell *et al.* 2001). ILB00 showed through numerical simulations that a stellar encounter may explain high orbital eccentricities and inclinations of outer Kuiper belt objects. They suggested that planetary formation was inhibited by the high orbital eccentricities and inclinations in the Kuiper belt while more inner region was almost intact and planetary formation proceeded, if the most effective stellar encounter with the proto-Solar system had pericenter distance ~ 150 -200AU. We perform more extensive calculations by both numerically and analytically to discuss the inhibition of planet formation in detail. Heggie and Rasio (1996) derived analytical formula for the change in eccentricity of binary stars by an encounter of a single passing star, using the Laplace-Runge-Lenz vector. In the limit of null mass of a binary companion, their formula is reduced to our analytical formula, although we used different method with the Gauss's equations (Brouwer and Clemence 1961). We derive the change in not only eccentricity but also inclination and study relative velocity of planetesimals taking into account the alignment of longitudes. in order to apply to planetary formation.

Heppenheimer (1978), Whitmire *et al.* (1998) and Marzari and Scholl (2000) study planet formation in a system with a binary companion orbiting outside a circumstellar disk around the primary star. The circumstellar disk is perturbed by the binary companion. They investigated relative velocity between planetesimals in the perturbed disk to find the condition of inhibition of planet formation, while we consider the effect of one passage of a field star.

In section 2, we briefly summarize critical velocity dispersions or critical eccentricities of planetesimals that are important to discuss planet accretion. In section3, we explain calculation models. In section 4, we show results of numerical simulations. The analytical formulae are derived in section 5. e and i pumped up by stellar perturbations in the weakly perturbed inner regime are explicitly given as functions of heliocentric radius and parameters of stellar encounters. Using the analytical formulae, in section 6, we discuss the size of planet forming region as a function of parameters of stellar clusters. We will show the radius of planet forming region is likely to be 40-60AU, in the case of a dense cluster, which may be consistent with the Solar system.

2. PLANETARY ACCRETION

Planetesimals with 1-10 km sizes are formed from dust grains in a protoplanetary disk through self-gravitational instability (e.g., Safronov 1969; Goldreich and Ward 1973) or sticking induced by turbulence of the disk gas (e.g., Weidenschilling and Cuzzi 1993). Accretion of the planetesimals make terrestrial planets and cores of jovian planets. The sticking (accretion) of planetesimals is caused by self-gravity. The accretion occurs, only when rebounding velocity of planetesimals after a collision is smaller than their surface escape velocity (v_{esc}). Since collision velocity is $\sim \sqrt{v_0^2 + v_{\text{esc}}^2}$ (Ohtsuki 1993), where v_0 is relative velocity of unperturbed crossing orbits neglecting mutual gravity, accretion occurs when $v_0 \lesssim v_{\text{esc}}$, except when too elastic or too inelastic cases (Ohtsuki 1993). If stellar encounters pump up v_0 more than v_{esc} , a collision between planetesimals results in disruption rather than accretion (e.g., Safronov 1969; Greenberg *et al.* 1978). Then planet formation is forestalled in this region. If the longitudes of pericenter and ascending node are randomly distributed, v_0 is nearly equal to velocity dispersion given by $v_d \sim \sqrt{e^2 + i} v_{\text{kep}}$ (e.g. Safronov 1969; Lissauer and Stewart 1993; Ohtsuki *et al.* 1993). As shown in section 6, the longitudes of the perturbed planetesimal orbits are not always random. We thus define “effective” eccentricity and inclination,

$$e_{\text{eff}} = |v_{0,xy}|/v_{\text{kep}}, \quad (1)$$

$$i_{\text{eff}} = |v_{0,z}|/v_{\text{kep}}, \quad (2)$$

where $v_{0,xy}$ and $v_{0,z}$ are the component on the initial disk and the vertical to the disk, respectively. By definition, $e_{\text{eff}} \lesssim e$ and $i_{\text{eff}} \lesssim i$. If the longitudes are aligned, $i_{\text{eff}} = 0$ and e_{eff} expresses small relative velocity due to shear motion.

The surface escape velocity of planetesimals with mass m and internal density ρ is

$$v_{\text{esc}} = \left(\frac{32\pi G^3 m^2 \rho}{3} \right)^{\frac{1}{6}}. \quad (3)$$

As shown in section 6, $e_{\text{eff}} \gtrsim i_{\text{eff}}$, so that $v_0 \sim e_{\text{eff}} v_{\text{kep}}$. The condition for a disruptive collision is $v_0 > v_{\text{esc}} = e_{\text{eff,crit}} v_{\text{kep}}$ (e.g., Stern 1995). The condition with effective eccentricity is

$$e_{\text{eff}} > e_{\text{eff,crit}} \simeq \left(\frac{32\pi m^2 a^3 \rho}{3M_1^3} \right)^{\frac{1}{6}}, \quad (4)$$

where a and M_1 are semimajor axis of a planetesimal and the mass of the host star, respectively. Numerically, $e_{\text{eff,crit}}$ is

$$e_{\text{eff,crit}} \sim 0.01 \left(\frac{m}{10^{22}\text{g}} \right)^{\frac{1}{3}} \left(\frac{\rho}{1\text{g/cm}^3} \right)^{\frac{1}{6}} \left(\frac{a}{10\text{AU}} \right)^{\frac{1}{2}}, \quad (5)$$

where the nominal value of $m \sim 10^{22}$ g corresponds to typical mass of Kuiper belt objects. In section 6, we show that the phase alignment breaks down for $e \gtrsim 0.01$, so that $e_{\text{eff}} \simeq e$ for $e \gtrsim 0.01$

and the condition (4) is no other than the condition for e . Equation (5) shows that e as small as 0.01 can significantly affect planetary accretion. If we consider “protoplanets” with lunar mass, $e_{\text{eff,crit}}$ is ~ 0.1 . However, it does not change the discussion on planet accretion in section 7.

3. CALCULATION MODEL AND BASIC EQUATION

We model a planetesimal disk as non-self-gravitating, collisionless particles that initially have coplanar circular orbits around a primary (host) star, because two-body relaxation time and mean collision time between planetesimals are much longer than an effective encounter time scale that is comparable to Kepler time scale at pericenter distance (D) of the encounter (for example, it is $\sim 10^3$ years for $D \sim 100\text{AU}$). We also neglect hydrodynamical gas drag, because the damping time due to the drag [$\simeq 10^7 (m/10^{22}\text{g})^{1/3} (e/0.1)^{-1}$ yr at 10AU (Adachi *et al.* 1976)] is longer than the effective encounter time $\sim 10^3$ years for $m > 10^{10}\text{g}$ at 10AU; we are considering planetesimals with much larger masses. The particulate disk encounters a hypothetical passing star. Note that the gravitational relaxation, collision and the drag can be important when we consider planet formation on a longer time scale after the stellar passing. The equation of motion of a planetesimal in the heliocentric frame (the frame with the primary star at center) is

$$\frac{d^2 \mathbf{r}_j}{dt^2} = -\frac{GM_1}{|\mathbf{r}_j|^3} \mathbf{r}_j + \frac{GM_2}{|\mathbf{R} - \mathbf{r}_j|^3} (\mathbf{R} - \mathbf{r}_j) - \frac{GM_2}{|\mathbf{R}|^3} \mathbf{R}, \quad (6)$$

where M_1 and M_2 are masses of the primary and the passing stars, \mathbf{r}_j and \mathbf{R} are position vectors of the planetesimal j and the passing star. The first term in the r. h. s. is force to produce Kepler motion around the primary star, and the second and third terms are direct and indirect perturbing forces of the passing star.

We scale length by pericenter distance D of the stellar encounter, mass by the primary star mass M_1 , and time by Ω_{kep}^{-1} where Ω_{kep} is Keplerian frequency at $a = D$ given by $\sqrt{GM_1/D^3}$. Equation (6) is then transformed to

$$\frac{d^2 \tilde{\mathbf{r}}_j}{d\tilde{t}^2} = -\frac{\tilde{\mathbf{r}}_j}{|\tilde{\mathbf{r}}_j|^3} - \frac{M_* (\tilde{\mathbf{r}}_j - \tilde{\mathbf{R}})}{|\tilde{\mathbf{r}}_j - \tilde{\mathbf{R}}|^3} - \frac{M_* \tilde{\mathbf{R}}}{|\tilde{\mathbf{R}}|^3}, \quad (7)$$

where $M_* = M_2/M_1$, $\tilde{\mathbf{r}}_j = \mathbf{r}_j/D$, $\tilde{\mathbf{R}} = \mathbf{R}/D$, and $\tilde{t} = \Omega_{\text{kep}} t$. Thus the parameters of encounters are inclination (i_*) relative to the initial planetesimal disk, eccentricity (e_*), and argument of perihelion (ω_*) of orbit of the passing star, and the scaled passing star mass (M_*). The encounter geometry is illustrated in Fig. 1. We calculate changes in e and i of the planetesimals according to Eq. (6) or (7) with various encounter parameters, through orbital integration and analytical estimation.

4. NUMERICAL SIMULATION

Regarding the method of numerical integration, we follow ILB00. We integrated orbits of 10,000 particles with surface number density $n_s \propto a^{-3/2}$. The particles are distributed in the region $a/D = 0.05-0.8$. Since we neglect mutual gravity and collisions of planetesimals, the particular choice of a -dependence of n_s and outer and inner edges of the disk does not affect the results. The initial e and i of particles are 0. We integrated Eq. (7), using a fourth order predictor-corrector scheme. Much more variations of encounter geometry, encounter velocity, and passing star mass were examined than ILB00 did.

Figures 2 show time evolution of e (left panels) and i (middle panels) and corresponding face-on snapshots (right panels) in the case with $e_* = 1$ (parabolic orbit), $i_* = 30^\circ$, $\omega_* = 0^\circ$, and $M_* = 1$. The (a) top, (b) middle and (c) bottom panels show snapshots at $\tilde{t} = -1.33, 0$ and 1.33 . The resultant e and i of planetesimals are mostly acquired when the passing star is near the pericenter.

The pumped-up e and i are shown in Fig. 3, as a function of the scaled initial semimajor axis a/D , in the case with $i_* = 5^\circ$ and $\omega_* = 90^\circ$. $(M_*, e_*) = (1,1), (0.2,1)$ and $(1,5)$ in Figs. 3a, 3b and 3c, respectively. In all cases, we find three characteristic regions of pumped-up e and i . In the inner region at $a/D \lesssim 0.1-0.3$, e and i are in proportion to $(a/D)^{5/2}$ and $(a/D)^{3/2}$, respectively. In the outer region at $a/D \gtrsim 0.1-0.3$, e and i have steeper a -gradient and divergence due to initial mean anomaly of planetesimals. In the outermost region, e of many planetesimals, is greater than 1, that is, the particles are ejected from the system. ILB00 also found these features. We find that $e \propto (a/D)^{5/2}$ and $i \propto (a/D)^{3/2}$ always hold. Analytical estimate derived in section 5 and Appendix reproduces $e \propto (a/D)^{5/2}$ and $i \propto (a/D)^{3/2}$. Note that the dashed lines with triangles are analytical estimate derived in section 5 and Appendix. Figures 3 show larger M_* and/or smaller e_* produce larger e and i . The agreement between the numerical and analytical results imply that e and i are scaled by $M_*/\sqrt{M_* + 1}$. The dependence on e_* is a more complicated form (see Appendix, Eqs. (46) to (49)).

Figures 4 show the dependence of i_* , in the case with $\omega_* = 0^\circ$, $e_* = 1$ and $M_* = 1$. i_* are 5° (Fig. 4a), 30° (Fig. 4b), 45° (Fig. 4c), 85° (Fig. 4d) and 150° (Fig. 4e). An encounter with $0^\circ < i_* < 90^\circ$ is a prograde encounter relative to rotation of the planetesimal disk and one with $90^\circ < i_* < 180^\circ$ is retrograde. The numerical results show i is dependent on i_* like $\propto \sin 2i_*$ in the inner region. Comparison between Figs. 4b and 4f suggest that e and i are the same between i_* and $90^\circ - i_*$ in the inner region, although retrograde encounters lead to less steep a/D -gradient than that in prograde encounters in the outer region ($a/D \gtrsim 0.1-0.3$). This shows that a secular effect is at work, so that we take the orbital average of the particle (Larwood 1997) in section 5. In Figs. 5 and 6, we show detailed dependence on i_* as well as ω_* . In the inner region, $e = e_0(a/D)^{5/2}$ and $i = i_0(a/D)^{3/2}$. We investigate the dependence of e_0 and i_0 on ω_* and i_* , in the case with $e_* = 1$ and $M_* = 1$. According to the analytical results (Eqs. (15) and (16) in section 5), we scale e_0 and i_0 by $(15\pi/32\sqrt{2})(1/\sqrt{2})$ and $(3\pi/8\sqrt{2})(1/\sqrt{2})$, respectively. We denote the scaled e_0 and i_0 by \tilde{e}_0 and \tilde{i}_0 . Figure 5a shows contours of numerically obtained \tilde{e}_0 as a function of i_* and ω_* .

The analytical result (Eq. 15) is plotted in Fig. 5b. We find dependence on ω_* is weaker than that on i_* . Since the analytical result shows that \tilde{i}_0 is independent of ω_* (Eq. 15), we plot \tilde{i}_0 as a function of i_* in Fig. 6. Filled circles in Fig. 6 show numerically obtained \tilde{i}_0 . We plot the numerical results of ten different ω_* for each i_* in Fig. 6. \tilde{i}_0 is almost completely independent of ω_* , which is consistent with the analytical result. Figures 5 and 6 show that the analytical results perfectly agree with numerical results. These figures show \tilde{e}_0 and \tilde{i}_0 are symmetric with respect to $i_* = 90^\circ$. Figure 6 clearly shows i is proportional to $\sin 2i_*$.

We next show the range of the power-law inner region is regulated by Ω_{kep} and Ω_* (ILB00 also discussed this issue), where $\Omega_{\text{kep}} = \sqrt{GM_1/a^3}$ and $\Omega_* = \sqrt{G(M_1 + M_2)(1 + e_*)/D^3}$ are the Keplerian frequency of a planetesimal with semimajor axis a and the angular velocity of the passing star at pericenter. Figures 3 and 4 show that if $\Omega_{\text{kep}} \gtrsim 5\Omega_*$ ($a/D \lesssim 0.2$ in case with $e_* = 1$ and $M_* = 1$), e is in proportion to $(a/D)^{2.5}$. If $\Omega_* \lesssim \Omega_{\text{kep}} \lesssim 5\Omega_*$ ($0.2 \lesssim a/D \lesssim 0.3$ in case with $e_* = 1$ and $M_* = 1$), e is pumped up most steeply. In this region, resonant interactions are important (Ostriker 1994). The condition of $n : 1$ commensurability is $\Omega_*/\Omega_{\text{kep}} = (a/D)^{3/2} \sqrt{(1 + M_*)(1 + e_*)} = 1/n$. For example, the 5:1, 4:1 and 3:1 resonances are at $a/D \simeq 0.21$, 0.25 and 0.30 in the case with $e_* = 1$, $M_* = 1$ and $0^\circ < i_* < 90^\circ$ (the prograde encounters; Figs. 4a to d). The resonances lower than 5:1 dominate non-resonant effects in this case. The 1:1, 2:1 and 3:1 are at $a/D \simeq 0.63$, 0.40 and 0.30 in the retrograde encounter (Fig. 4e). In the retrograde cases, resonances occur with particles in the far side of the disk, so that their effects are relatively weak. Numerical simulations suggest that the boundary between the inner and outer regions is at the 5:1 commensurability, $a/D \simeq [(1 + M_*)(1 + e_*)]^{-1/3} (1/5)^{2/3}$, in the case of prograde encounters and at the 3:1, $a/D \simeq [(1 + M_*)(1 + e_*)]^{-1/3} (1/3)^{2/3}$, in the case of retrograde encounters. Ostriker (1994) analytically derived consistent conditions. If $\Omega_{\text{kep}} \lesssim \Omega_*$ ($a/D \gtrsim 0.63$ in case with $e_* = 1$ and $M_* = 1$), there is no Lindblad resonance, so that a -gradient is less steep than that in the resonant region.

In the outer and outermost regions, pumped-up e and i depend not only on initial radial position but also on azimuthal position of planetesimals. In the case of a prograde encounter, particles in the near side of the disk at pericenter passage are affected by resonances while ones in the far side are hardly affected. In these region, Ω_{kep} is not large enough compared with Ω_* , so that such asymmetry remains. In the case of a retrograde encounter, only far-side planetesimals are affected. Note that particles with very small e and i exist at resonant points depending on the azimuthal position, which might be able start runaway accretion (section 6).

The change in semimajor axis, $\Delta a/a$, is much smaller than that in e and i (in radian) in the inner region, as shown by comparison of Fig. 3a and Fig. 7. In the inner region, $\Omega_{\text{kep}} \gg \Omega_*$, so that for particles there gravitational potential of the passing star is quasi-stationary. In the stationary potential, energy and hence a is conserved. Since the potential is not axisymmetric in the heliocentric frame, e is changed. Since it is inclined from the orbital plane of the particles, i is also changed. In the outer and outermost regions with $\Omega_* \sim \Omega_{\text{kep}}$, change in $\Delta a/a$ can not be neglected compared with that in e or i .

A stellar encounter can cause disk truncation. Many particles are unbound ($e \gtrsim 1$) at $a/D \gtrsim 0.3$ after the prograde encounter, in the case with $M_* = 1$, $e_* = 1$ (Fig. 2c). Some particles are captured by the passing star during a prograde encounter. Their eccentricities are usually close to unity in the frame in which the passing star is at center. (If the passing star also has a planetesimal disk, some planetesimals are captured by the primary star.) Note that exact amount of the disk truncation and the capture depends on the radius of outer edge of the disk relative to D . Such strong encounters would have many interesting features as mentioned in Section 1. However, as shown in section 2, in order to discuss the effects on planet accretion, the regimes of e , $i \sim 0.01$ are important. The pumped-up e and i in such regimes are near the inner region. Hence, analytical linear calculations would well predict the effects on planet accretion.

5. ANALYTICAL CALCULATION

We derive analytical formulae of pumped-up e and i in the inner region. Orbital integrations show that in that region, $e = e_0(a/D)^{5/2}$ and $i = i_0(a/D)^{3/2}$. The analytical formulae explain these dependence on (a/D) as well as dependence of e_0 and i_0 on M_* , i_* , ω_* and e_* . Heggie and Rasio (1996) derived change in eccentricity of binary stars which encounter a passing single star, using the Laplace-Runge-Lenz vector. Using the Gauss's equations, we derive change in inclination as well as eccentricity. In the limit of null mass of a binary companion, the formula by Heggie and Rasio (1996) is equivalent to our formula for eccentricity. The analytical results show the phase alignment, so that e and i do not necessarily determine relative velocity between perturbed planetesimals. We numerically study the degree of the phase alignment in section 6.

We are mostly concerned with parabolic encounters ($e_* = 1$), since for encounters we are interested in, e_* is not far from 1, as follows. (We also calculate hyperbolic encounters ($e_* > 1$) with the same analytic method in Appendix.) The specific angular momentum (l_*) and specific energy (E_*) of the passing star orbit relative to the primary star are $\sim v_* D \sim \sqrt{v_{*d}^2 + [v_{\text{kep}}(D)]^2} \times D$ and $v_{*d}^2/2$, respectively, where v_{*d} is velocity dispersion of stars in a cluster. Thereby, $e_* = \sqrt{1 + 2l_*^2 E_*/G^2(M_1 + M_2)^2} \sim \sqrt{1 + (v_{*d}/v_{\text{kep}})^2 [1 + (v_{*d}/v_{\text{kep}})]^2}$. Since v_{*d} is ~ 1 km/s (Binney and Tremaine 1987) and $v_{\text{kep}}(D)$ is larger than 1 km/s for $D \lesssim 1000\text{AU}$, which we are interested in, e_* is ~ 1 .

We adopt the following approximations to derive pumped-up e and i in the inner region.

- (i) $\Delta a/a$ is neglected, since $\Delta a/a \ll e, i$,
- (ii) orbital averaging is applied for planetesimal orbits, since $\Omega_{\text{kep}} \gg \Omega_*$ (Larwood 1997),
- (iii) $e, i, a/D \ll 1$.

In the equation of motion of a planetesimal given by Eq. (6), the second and third terms in

the r. h. s. stand for the perturbation forces of the passing star. We define

$$\mathbf{F}_{\text{perturb}} = \frac{GM_2}{|\mathbf{R} - \mathbf{r}|^3}(\mathbf{R} - \mathbf{r}) - \frac{GM_2}{|\mathbf{R}|^3}\mathbf{R}. \quad (8)$$

We divide the perturbation force into r , θ , and z components,

$$\mathbf{F}_{\text{perturb}} = \bar{R}\mathbf{e}_r + \bar{T}\mathbf{e}_\theta + \bar{N}\mathbf{e}_z, \quad (9)$$

where \mathbf{e}_r ($= \mathbf{r}/|\mathbf{r}|$), \mathbf{e}_θ and \mathbf{e}_z are unit vectors in the radial, tangential, and normal components in initial orbital plane of the planetesimal disk, respectively. We define $h = e \sin(\omega + \Omega)$, $k = e \cos(\omega + \Omega)$, $p = \sin i \sin \Omega$ and $q = \sin i \cos \Omega$, where ω and Ω are the argument of pericenter and longitude of ascending node of a planetesimal. The equations of motion with these orbital elements in $h, k, p, q \ll 1$ ($e, i \ll 1$: assumption (iii)), which are called Gauss's equations, are (Brouwer and Clemence 1961)

$$\frac{dh}{dt} \simeq \sqrt{\frac{a}{GM_1}}(-\bar{R} \cos \theta + 2\bar{T} \sin \theta), \quad (10)$$

$$\frac{dk}{dt} \simeq \sqrt{\frac{a}{GM_1}}(\bar{R} \sin \theta + 2\bar{T} \cos \theta), \quad (11)$$

$$\frac{dp}{dt} \simeq \sqrt{\frac{a}{GM_1}}\bar{N} \sin \theta, \quad (12)$$

$$\frac{dq}{dt} \simeq \sqrt{\frac{a}{GM_1}}\bar{N} \cos \theta, \quad (13)$$

where $\theta = f + \omega + \Omega$ (f is true anomaly) and we retained the lowest order terms of e and i in the right hand side.

We expand \bar{R} , \bar{T} , \bar{N} in terms of a/D up to the terms of $(a/D)^2$ (see Appendix, Eqs.(37), (38), and (39)). Corresponding to assumption (ii), we take orbital averaging, e.g.,

$$\left\langle \frac{dh}{dt} \right\rangle = \frac{\int_0^{2\pi} (dh/dt) d\theta}{2\pi}. \quad (14)$$

The averaged dh/dt , dk/dt , dp/dt and dq/dt are shown in Eqs. (41), (42), (43) and (44) in Appendix. Finally, we integrate them with the stellar passage, assuming constant a of planetesimals (assumption (i)) to obtain changes in h , k , p , and q caused by the stellar passage in parabolic orbit (Appendix, Eqs. (46) to (49)).

Since we start with $h, k, p, q = 0$, their changes are equal to final h , k , p , and q of planetesimals. Since $e = \sqrt{h^2 + k^2}$ and $i = \sqrt{p^2 + q^2}$, we obtain final e and i as

$$e \simeq \frac{15\pi}{32\sqrt{2}} \frac{M_*}{\sqrt{1+M_*}} \left(\frac{a}{D}\right)^{\frac{5}{2}} \times \left[\cos^2 \omega_* \left(1 - \frac{5}{4} \sin^2 i_*\right)^2 + \sin^2 \omega_* \cos^2 i_* \left(1 - \frac{15}{4} \sin^2 i_*\right)^2 \right]^{\frac{1}{2}}, \quad (15)$$

$$i \simeq \frac{3\pi}{8\sqrt{2}} \frac{M_*}{\sqrt{1+M_*}} \left(\frac{a}{D}\right)^{\frac{3}{2}} |\sin 2i_*|, \quad (16)$$

$$\tilde{\omega} \simeq \arctan \left[-\frac{\cos \omega_* (5 \cos^2 i_* - 1)}{\sin \omega_* \cos i_* (15 \cos^2 i_* - 11)} \right], \quad (17)$$

$$\Omega \simeq \begin{cases} \pi/2 & \text{for } 0^\circ \leq i_* \leq 90^\circ, \\ -\pi/2 & \text{for } 90^\circ < i_* \leq 180^\circ, \end{cases} \quad (18)$$

where $\tilde{\omega}$ is the longitude of pericenter and $= \omega + \Omega$. The detailed derivation is shown in Appendix. We have analytically explained the power-law dependence of pumped-up e and i on (a/D) in inner region. Since the orbital averaging is valid, $\tilde{\omega}$ and Ω of the perturbed orbit do not depend on azimuthal position of a planetesimal as Eqs. (17) and (18). Such phase alignment of planetesimals' orbits, leads to reduction of the colliding velocity between planetesimals (section 6).

We plot the analytical formulae (15) and (16) with dashed lines with triangles in Figs. 3 and 4. e_0 ($= e/(a/D)^{5/2}$) and i_0 ($= i/(a/D)^{3/2}$) of the analytical formulae are showed in Figs. 5b and 6. The analytical formulae show excellent agreement with the numerical results in the inner power-law inner region. We examined the agreement in the cases with other parameters and found that the difference is always less than a factor 2.

The pumped-up e and i depend on phase angles i_* and ω_* of a stellar encounter. The average of e and i with ω_* and i_* is

$$e_{\text{ave}} = \left[\frac{1}{4\pi} \int_0^{2\pi} d\omega_* \int_0^\pi di_* (\sin i_*) e^2 \right]^{\frac{1}{2}} = \frac{15\pi}{32\sqrt{7}} \frac{M_*}{\sqrt{1+M_*}} \left(\frac{a}{D}\right)^{\frac{5}{2}}, \quad (19)$$

$$i_{\text{ave}} = \left[\frac{1}{4\pi} \int_0^{2\pi} d\omega_* \int_0^\pi di_* (\sin i_*) i^2 \right]^{\frac{1}{2}} = \frac{\sqrt{15}\pi}{20} \frac{M_*}{\sqrt{M_*+1}} \left(\frac{a}{D}\right)^{\frac{3}{2}}. \quad (20)$$

We use e_{ave} and i_{ave} to estimate the boundary of planet accretion in section 7.

Ostriker (1994) analytically investigated the change in energy (ΔE_{disk}) and perpendicular angular momentum ($\Delta L_{\text{disk},z}$) of an entire circumstellar disk during a parabolic stellar encounter. Although the author was concerned mainly with resonant region for $r_{\text{disk,max}} \gtrsim 0.2D$, the author presented phase-averaged approximate $\Delta L_{\text{disk},z}$ (but not ΔE_{disk}) for $r_{\text{disk,max}} \lesssim 0.2D$ (non-resonant region). Since specific perpendicular angular momentum ΔL_z are written by $L_0(\Delta a/a - \Delta e^2 - \Delta i^2)/2$ where L_0 is the initial angular momentum, $\Delta L_{\text{disk},z}$ is obtained by integrating ΔL_z over radius from $r_{\text{disk,min}}$ to $r_{\text{disk,max}}$, using our results in the power-law inner region. Our $\Delta L_{\text{disk},z}$ is larger by a factor $\sim \mathcal{O}(10)$ than the author's with less steep a -gradient.

Heggie and Rasio (1996) derived formula of change in eccentricity of binary stars after a single passing encounter. To derive this formula, they use the Laplace-Runge-Lenz vector. Their formula of change in eccentricity of binary stars with circular orbit is perfectly the same as our formula derived by a different method, in limit of null mass of a binary companion.

6. RELATIVE VELOCITY

As shown in the last section, difference of $\tilde{\omega}$ or Ω between planetesimals are almost 0 as long as the linear analysis is valid. We investigate the relative velocity between planetesimals after a stellar passing, using the numerical data. Figure 8 show that $\tilde{\omega}$ and Ω after the stellar encounter with $(i_*, \omega_*, M_*, e_*) = (5^\circ, 90^\circ, 1, 1)$. $\tilde{\omega}$ and Ω are aligned in the region where e and i have the power law radial dependence. In the outer region where the resonances are important, $\tilde{\omega}$ is randomly distributed (Retrograde encounters show similar results).

Whitmire *et al.* (1998) evaluated relative velocities between planetesimals whose orbits are crossing assuming coplanar orbits. Extending their method to three-dimension with assumption $i \lesssim 1$ (radian), we evaluated the relative velocity between planetesimals 1 and 2. For $i \lesssim 1$, the projective orbit of a planetesimal on the initial disk is almost the same as the case with $i = 0$. We calculate the relative velocity, if $|z_1 - z_2|$ is smaller than the sum of planetesimal radii at the point where the projective orbits are crossing, where $z_{1(2)}$ is position vertical to the initial disk. The component on the initial disk $v_{0,xy}$ and that vertical to the disk $v_{0,z}$ at a crossing point are

$$v_{0,xy}^2 = GM_1 \left[\frac{e_1 \sin(f_2 - \Delta\tilde{\omega})}{\sqrt{p_1}} - \frac{e_2 \sin f_2}{\sqrt{p_2}} \right]^2 + \left[\frac{\sqrt{p_1}}{r} - \frac{\sqrt{p_2}}{r} \right]^2, \quad (21)$$

$$v_{0,z} = \sqrt{GM_1} \left| \frac{i_1 [\cos(f_2 - \Delta\tilde{\omega} + \omega_1) + e_1 \cos \omega_1]}{\sqrt{p_1}} - \frac{i_2 [\cos(f_2 + \omega_2) + e_2 \cos \omega_2]}{\sqrt{p_2}} \right|, \quad (22)$$

where $p_{1(2)} = a_{1(2)}(1 - e_{1(2)})$, $\Delta\tilde{\omega}$ and $\Delta\Omega$ are $\tilde{\omega}_2 - \tilde{\omega}_1$ and $\Omega_2 - \Omega_1$. f_2 is true anomaly of planetesimal 2 at the crossing point, satisfying

$$\cos f_2 = \frac{-AB \pm C\sqrt{C^2 + B^2 - A^2}}{B^2 + C^2} \quad (23)$$

where

$$A = p_2 - p_1, \quad (24)$$

$$B = e_1 p_2 \cos \Delta\tilde{\omega} - e_2 p_1, \quad (25)$$

$$C = e_1 p_2 \sin \Delta\tilde{\omega}. \quad (26)$$

r is radial position of planetesimals at the crossing point, given by

$$r = \frac{P_2}{1 + e_2 \cos f_2}. \quad (27)$$

In Fig. 9, e and i are compared with $e_{\text{eff}} = v_{0,xy}/v_{\text{kep}}$ and $i_{\text{eff}} = v_{0,z}/v_{\text{kep}}$, which are calculated through Eqs. (21) and (22) with the data in Fig. 8. We also plot

$$e_{\text{rel}} \equiv |\mathbf{e}_2 - \mathbf{e}_1| = e_1^2 + e_2^2 - 2e_1 e_2 \cos \Delta\omega, \quad (28)$$

$$i_{\text{rel}} \equiv |\mathbf{i}_2 - \mathbf{i}_1| = i_1^2 + i_2^2 - 2i_1 i_2 \cos \Delta\Omega, \quad (29)$$

where $\mathbf{e}_j \mathbf{i}_j$ ($j = 1, 2$) are $(e_j \cos \tilde{\omega}_j, e_j \sin \tilde{\omega}_j)$ and $(i_j \cos \Omega_j, i_j \sin \Omega_j)$. In Fig. 9, we found $e_{\text{rel}} \simeq e_{\text{eff}}$ and $i_{\text{rel}} \simeq i_{\text{eff}}$. The effect of the phase alignment is more clear with e_{rel} and i_{rel} rather than with e_{eff} and i_{eff} , because e_{rel} and i_{rel} are directly related with $\Delta\tilde{\omega}$ and $\Delta\Omega$. A stellar encounter results in alignment of $\tilde{\omega}$ and Ω ($\Delta\tilde{\omega} \simeq 0$ and $\Delta\Omega \simeq 0$) in inner region, e_{eff} (e_{rel}) $\ll e$ and i_{eff} (i_{rel}) $\ll i$. In outer region, the linear approximation breaks down and $\Delta\tilde{\omega}$ and $\Delta\Omega$ are randomly distributed, so that $e_{\text{rel}} \simeq e$ and $i_{\text{rel}} \simeq i$. Figure 8 shows that the alignment breaks down at $a/D \sim 0.2$ for $\tilde{\omega}$, and ~ 0.3 for Ω , resulting in more rapid increase in e_{rel} with a than i_{rel} . As a result, at $e_{\text{eff}} \sim e_{\text{eff,crit}} \sim 0.01$, $e_{\text{eff}} \sim e > i_{\text{eff}}$. Also for other encounter parameters, we find a similar trend. We thus estimate planet formation region, using Eqs. (5) and (15) with $e_{\text{eff}} \sim e$.

In Fig. 9, we also find that at a resonant point ($a/D \simeq 0.2$), all of e and e_{eff} have wide variety of values caused by the resonant feature. Although many planetesimals have e_{eff} well beyond $e_{\text{eff,crit}}$, but some fraction has $e_{\text{eff}} \ll e_{\text{eff,crit}}$ should be very fast. If it can precede disruption due to collisions with high e_{eff} planetesimals to form large bodies with high $e_{\text{eff,crit}}$ quickly, planet can be formed at this particular resonant point.

We also study the cases with non-zero initial e and i because self-gravity of planetesimals or more distant stellar encounters would occur before the strongest encounter. Figure 10 shows the e , i , $\tilde{\omega}$ and Ω of planetesimals after the encounter with initial e and $i = 1 \times 10^{-4}$. $\tilde{\omega}$ and Ω are initially at random. The encounter parameters are $(i_*, \omega_*, M_*, e_*) = (5^\circ, 90^\circ, 1, 1)$. If change of e and i by the encounter are much larger than the initial e and i , the features of e and i are almost the same as those in the case of initial e and $i = 0$; $\tilde{\omega}$ and Ω are aligned. If the pumped-up e and i are smaller than the initial e and i , $\tilde{\omega}$ and Ω remain at random.

After the stellar encounter, self-gravity of planetesimals, collision between them and gas drag would be important for accretion of planetesimals on a longer time scale. They may keep the phase alignment rather than destroy it (e.g., Goldreich and Tremaine 1982; Marzari and Scholl 2000; Ito and Tanikawa 2001), until a strong perturber such as a giant planet is formed. We need more study about these effects on planetesimal accretion.

7. SIZE OF A PLANET FORMING REGION

In the last section, we have derived analytical expressions for e and i pumped up by a passing stellar encounter. The expressions perfectly agree with numerical calculations in the region $e \lesssim 0.01$. In this section, we estimate the size of planet forming region in a protoplanetary disk, using these analytical expressions.

According to the argument in the last section, the collision between planetesimals results in disruption rather than accretion (Eq. (5)),

$$e_{\text{eff}} > \frac{v_{\text{esc}}}{v_{\text{kep}}} \sim 0.01 \left(\frac{m}{10^{22}\text{g}} \right)^{\frac{1}{3}} \left(\frac{a}{10\text{AU}} \right)^{\frac{1}{2}}, \quad (30)$$

where m is mass of a planetesimal. For $e \gtrsim 0.01$, $\tilde{\omega}$ and Ω are not aligned and $e \simeq e_{\text{eff}}$.

As shown in sections 3 and 4, the radial gradient of e is so steep that there is a sharp boundary of the disk that divides the planet forming region and the disruptive region where planet formation is inhibited. Since e_{eff} , which includes the effect of the phase alignment, has steeper gradient than e , the actual boundary should be sharper. Here we derive the radius of the boundary as a function of physical parameters of the stellar cluster which the host star of the planetary system belonged to.

In the case with $e \gtrsim 0.01$, the analytical expressions slightly underestimate the pumped-up e , since resonant effects are also important in this case. However, we can use them to estimate the boundary radius, because the radial gradient of e is so steep that the underestimation hardly changes the boundary radius.

In a stellar cluster, $e_* \sim 1$, as mentioned in Section 5. Substituting Eq. (19) into Eq. (5), we obtain the boundary radius a_{planet} as

$$a_{\text{planet}} \sim 40 \left(\frac{m}{10^{22}\text{g}} \right)^{\frac{1}{6}} \left(\frac{F}{2} \right)^{\frac{1}{4}} \left(\frac{D}{150\text{AU}} \right)^{\frac{5}{4}} \text{AU}, \quad (31)$$

where $F = M_* + 1/M_*^2$. If M_* is 1, F is 2. The factor $(F/2)^{1/4}$ can not significantly deviate from 1. The dependence of m on a_{planet} is also very weak. Therefore, a_{planet} depends almost only on D . A stellar encounter with $D \sim 150\text{-}200\text{AU}$ restricts the disk radius of a planetary system (the disk radius of planet forming region) to 40-60AU.

Considering evaporation process of a stellar cluster, Adams and Laughlin (2001) estimated effective D before the evaporation as

$$D \sim 200 \left(\frac{R_{\text{cluster}}}{2\text{pc}} \right) \left(\frac{N}{2000} \right)^{-1} \text{AU}, \quad (32)$$

where N is number of stars in a stellar cluster and R_{cluster} is size of the cluster. For the Trapezium cluster in Orion, $N \sim 2300$ and $R_{\text{cluster}} \sim 2 \text{ pc}$. In a dense cluster like Orion Trapezium, D is as small as 200AU, so that $a_{\text{planet}} \sim 40\text{-}60\text{AU}$. ILB00 demonstrated that the high eccentricity and inclination of objects in the outer Kuiper Belt may be explained by the stellar encounter with $D \sim 150\text{-}200\text{AU}$, which may suggest the Sun was born in a dense stellar cluster.

So far, we have only considered passing of a single star, however, passing of binary stars would also be important. Laughlin and Adams (1998) and Adams and Laughlin (2001) (also see the next section) suggested that passing binary encounters are more disruptive than passing single-star encounters. If we take into account the effects of passing binary encounters, a_{planet} may be smaller than Eq. (31).

We should investigate distribution of D (not only an effective value) as well as the effects of passing binary encounters, to discuss diversity of sizes of planetary systems in more detail.

Note that as discussed in the last section, less than planetesimals might coalesce with each other, resulting in a kind of runaway growth; planets might be formed at particular resonant location beyond a_{planet} .

8. CONCLUSION & DISCUSSION

We have investigated the effects of a passing stellar encounter on a planetesimal disk through orbital integration and analytical calculations. Since stars are generally born as members of a cluster and would stay in the cluster on timescales more than 10^8 years (Kroupa 1995; 1998), a relatively close encounter, e.g., one with distance $\sim 200\text{AU}$ is likely to occur during formation age of a planetary system.

We considered that a disk of massless particles (planetesimals) orbiting a primary star encounters a passing single star. Encounter parameters are pericenter distance of the encounter (D), the argument of perihelion (ω_*), eccentricity (e_*) and inclination (i_*) of the orbit of the passing star, and the mass ratio (M_*) of the passing star’s mass to the primary one. We showed that the pumped-up orbital eccentricities e and inclinations i of planetesimals have steep radial gradient. In the inner region at semimajor axis $a \lesssim \alpha [(1 + M_*)/2]^{1/3} [(1 + e_*)/2]^{1/3} D$, ($\alpha \simeq 0.2$ for a prograde encounter and $\alpha \sim 0.3$ for a retrograde encounter) $e \propto (a/D)^{5/2}$ and $i \propto (a/D)^{3/2}$, independent of the encounter parameters. The result is also independent of initial azimuthal position of planetesimals, because orbital period of planetesimals is much shorter than passing time scale.

In the outer region $a \gtrsim \alpha [(1 + M_*)/2]^{1/3} [(1 + e_*)/2]^{1/3} D$, the radial gradient is steeper, but is not expressed by a single power-law. In this region, resonant effects are more important (Ostriker 1994).

The longitude of pericenter $\tilde{\omega}$ and ascending node Ω are aligned between planetesimals, in power-law region of e and i (Fig. 8). We investigated relative velocity between planetesimals whose orbits cross. We define $e_{\text{eff}} = v_{0,xy}/v_{\text{kep}}$ and $i_{\text{eff}} = v_{0,z}/v_{\text{kep}}$ where $v_{0,xy}$ and $v_{0,z}$ are planar and vertical components of the relative velocity. We found that e_{eff} and i_{eff} are smaller than e and i by many orders of magnitude. In outer region, the phase alignment brake down, so that $e \sim e_{\text{eff}}$ and $i \sim i_{\text{eff}}$.

The stellar perturbations significantly affect the outer part of a planetesimal disk. Even in the inner disk, e_{eff} and i_{eff} that are pumped up to $\gtrsim 0.01$ inhibit further planetesimal accretion, because the relative velocity corresponding to $e_{\text{eff}}, i_{\text{eff}} \gtrsim 0.01$ exceeds the surface escape velocity of planetesimals and collisions between planetesimals should be disruptive. We investigate the relatively weakly perturbed region with $e, i \sim 0.01$ to study the effects on planetesimal accretion. We have derived analytical expressions of e and i in the power-law inner region.

With the approximations of constant the semimajor axis a and orbit averaging of planetesimals’ motion, we derived analytical expressions of the pumped-up e and i (Eqs. (15) and (16)) in the

case with a parabolic encounter ($e_* = 1$) as

$$e \simeq \frac{15\pi}{32\sqrt{2}} \frac{M_*}{\sqrt{M_* + 1}} \left(\frac{a}{D}\right)^{5/2} \times \left[\cos^2 \omega_* \left(1 - \frac{5}{4} \sin^2 i_*\right)^2 + \sin^2 \omega_* \cos^2 i_* \left(1 - \frac{15}{4} \sin^2 i_*\right)^2 \right]^{1/2}, \quad (33)$$

$$i \simeq \frac{3\pi}{8\sqrt{2}} \frac{M_*}{\sqrt{M_* + 1}} \left(\frac{a}{D}\right)^{3/2} |\sin 2i_*|. \quad (34)$$

Note that the dependence on ω_* is weak in both expressions and that on i_* is also weak in the former expression (Figs. 5 and 6). The analytical formulae agree with the numerical results within a factor 2. We also calculated e and i in the case with a hyperbolic encounter ($e_* > 1$) in Appendix.

At $e_{\text{eff}} \sim 0.01$, $e \sim e_{\text{eff}}$ and e_{eff} is larger than i_{eff} , because the phase alignment for $\tilde{\omega}$ breaks down at smaller a than that for Ω . Hence the relative velocity is regulated by e at $e_{\text{eff}} \sim 0.01$ and disruptive collisions $e \gtrsim e_{\text{eff,crit}}$ where $e_{\text{eff,crit}}$ is given as Eq. (5). Since the radial gradient of e and e_{eff} are so steep that there is a sharp boundary in the disk that divides the planet forming region and the disruptive region where planet formation is inhibited. Planetesimal orbits are significantly modified beyond the boundary, while they are almost intact inside the boundary. We derived the boundary radius (a_{planet}) by the condition that the pumped-up velocity dispersion of planetesimals is equal to their surface escape velocity (Eq.(31)):

$$a_{\text{planet}} \sim 40 \left(\frac{m}{10^{22}\text{g}}\right)^{1/6} \left(\frac{F}{2}\right)^{1/4} \left(\frac{D}{150\text{AU}}\right)^{5/4} \text{AU}, \quad (35)$$

where $F \simeq M_* + 1/M_*^2$ and m is planetesimal mass. The variation of $(F/2)^{1/4}$ is small. The dependence of a_{planet} on m is very weak. Thereby a_{planet} depends almost only on D . In a dense cluster like Orion Trapezium, D is as small as 200AU (Adams and Laughlin 2001). Such a stellar encounter with 150-200AU restricts the disk radius of a planetary system (the disk radius of planet forming region) to 40-60AU.

In the Solar system, there would be no planetary-sized object beyond Neptune at 30AU. Kuiper-belt objects beyond Neptune have velocity dispersion considerably larger than their surface escape velocity. These might be accounted for by a stellar encounter in a dense stellar (ILB00; Adams & Laughlin 2001). Our Solar system may have belonged to a dense stellar in the formation age.

In a dense stellar cluster, planetary systems cannot be significantly larger than the size of the planetary region of our Solar system (~ 30 -40AU). To discuss diversity of sizes of planetary systems in detail, we will need to investigate distribution of D (not only an effective value). In the present paper, we have only considered passing of a single star, however, passing of binary stars would also be important. Laughlin and Adams (1998; 2000) suggested that passing binary encounters are more disruptive than passing single-star encounters. We performed several runs of passing close

binary stars. If the total binary mass is equal to a single passing star mass, the results show that the encounter of close binary stars is similar to the single stellar encounter, except that e is pumped up more highly at some resonant positions corresponding to the binary frequency even in the inner region. As long as close binary cases are considered, a_{planet} may be estimated with the single star's equation using binary total mass.

The effects of cumulative distant (large D) encounters may be neglected compared with a few closest encounters. The successive distant encounters change h, k, p, q defined in section 5 constructively or destructively, so that their averages would be zero. Their dispersions depend on D with large negative power-indexes (< -3), so that the cumulative effects integrated by $2\pi D dD$ would quickly vanish with D .

Circumstellar dust disks around stars are observed. This dust may be secondary, because dust would be removed before stellar age, by radiative pressure and pointing Robertson effect (e.g., Artymowicz 1997; Backman and Paresce 1993). Disruptive collisions at $a > a_{\text{planet}}$ would continuously produce dust materials, which might form dust-debris disks around Vega-like stars. On the other hand, planetesimals grow to be large bodies at $a < a_{\text{planet}}$, not producing dust materials. Although radiative pressure and pointing Robertson effect would cause migration of the produced dust materials (e.g., Artymowicz 1997; Backman and Paresce 1993), a_{planet} correspond to the radius of inner holes of dust-debris disks. The radii of the observed inner holes around ϵ Eridani (Greaves *et al.* 1998), HD 14156 (Andrillat *et al.* 1990; Sahu *et al.* 1998; Augereau *et al.* 1999; Weinberger *et al.* 1999; 2000), HD 207129 (Jourdain de Muizon *et al.* 1999) and HR 4796A (Jura *et al.* 1995; Fajardo-Acosta *et al.* 1998; Jayawardhana *et al.* 1998) are 30-100AU, which are comparable to a_{planet} in the case of relatively dense clusters. We need more detailed analysis of distribution of a_{planet} as a function of environment parameters of stellar clusters, combined with discussions of collision outcomes and migration processes of dust materials, to discuss the diversity of inner holes of dust-debris disks.

Appendix

We integrate Eqs. (10), (11), (12) and (13) and derive expressions of e and i pumped up by a passing star as functions of a/D , M_* , ω_* , e_* and i_* .

$\mathbf{F}_{\text{perturb}}$ defined by Eq. (8) is expanded as a series of a/D up to the order $(a/D)^2$:

$$\mathbf{F}_{\text{perturb}} \simeq \frac{GM_2}{R^3} \left[\left(3 \frac{\mathbf{R} \cdot \mathbf{e}_r}{R} \mathbf{R} - R \mathbf{e}_r \right) \left(\frac{a}{R} \right) + \left\{ \left(\frac{15}{2} \frac{(\mathbf{R} \cdot \mathbf{e}_r)^2}{R^2} - \frac{3}{2} \right) \mathbf{R} - 3(\mathbf{R} \cdot \mathbf{e}_r) \mathbf{e}_r \right\} \left(\frac{a}{R} \right)^2 \right], \quad (36)$$

where $R = |\mathbf{R}|$ and $\mathbf{e}_r = \mathbf{r}/a$. We denote $\mathbf{F}_{\text{perturb}} = \bar{R} \mathbf{e}_r + \bar{T} \mathbf{e}_\theta + \bar{N} \mathbf{e}_z$, where \mathbf{e}_θ and \mathbf{e}_z are unit vectors in the tangential and vertical directions. We denote that $\mathbf{e}_r = (\cos \theta, \sin \theta, 0)$ and $\mathbf{R} = (R_x, R_y, R_z)$ in the Cartesian coordinates where the initial planetesimal disk is on the x - y plane and the x -axis is directed to ascending node of the passing star's orbit. The components,

\bar{R} , \bar{T} and \bar{N} are

$$\bar{R} \simeq \frac{GM_2}{R^3} \left[\left(3 \frac{(\mathbf{R} \cdot \mathbf{e}_r)^2}{R} - R \right) \left(\frac{a}{R} \right) + \left\{ \left(\frac{15}{2} \frac{(\mathbf{R} \cdot \mathbf{e}_r)^2}{R^2} - \frac{9}{2} \right) \mathbf{R} \cdot \mathbf{e}_r \right\} \left(\frac{a}{R} \right)^2 \right], \quad (37)$$

$$\bar{T} \simeq \frac{GM_2}{R^3} \left[3 \frac{(\mathbf{R} \cdot \mathbf{e}_r)}{R} \phi \left(\frac{a}{R} \right) \left\{ \left(\frac{15}{2} \frac{(\mathbf{R} \cdot \mathbf{e}_r)^2}{R^2} - \frac{3}{2} \right) \phi \right\} \left(\frac{a}{R} \right)^2 \right], \quad (38)$$

$$\bar{N} \simeq \frac{GM_2}{R^3} \left[3 \frac{(\mathbf{R} \cdot \mathbf{e}_r)}{R} R_z \left(\frac{a}{R} \right) + \left(\frac{15}{2} \frac{(\mathbf{R} \cdot \mathbf{e}_r)^2}{R^2} - \frac{3}{2} \right) R_z \left(\frac{a}{R} \right)^2 \right], \quad (39)$$

where ϕ is z component of $\mathbf{e}_r \times \mathbf{R}$.

Substituting Eqs. (37), (39), and (38) into Eqs. (10), (11), (12) and (13) and taking the orbit averaging, e.g.,

$$\left\langle \frac{dh}{dt} \right\rangle = \frac{\int_0^{2\pi} (dh/dt) d\theta}{2\pi}, \quad (40)$$

where “ $\langle \ \rangle$ ” means the orbit averaging, we obtain

$$\left\langle \frac{dh}{dt} \right\rangle \simeq -\frac{GM_2}{R^3} \sqrt{\frac{a}{GM_1}} R_x \left[\frac{75}{16} \frac{R_x^2 + R_y^2}{R^2} - \frac{15}{4} \right] \left(\frac{a}{R} \right)^2, \quad (41)$$

$$\left\langle \frac{dk}{dt} \right\rangle \simeq \frac{GM_2}{R^3} \sqrt{\frac{a}{GM_1}} R_y \left[\frac{75}{16} \frac{R_x^2 + R_y^2}{R^2} - \frac{15}{4} \right] \left(\frac{a}{R} \right)^2, \quad (42)$$

$$\left\langle \frac{dp}{dt} \right\rangle \simeq \frac{GM_2}{R^3} \sqrt{\frac{a}{GM_1}} R_y \left[\frac{3}{2} \frac{R_z}{R} \right] \left(\frac{a}{R} \right), \quad (43)$$

$$\left\langle \frac{dq}{dt} \right\rangle \simeq \frac{GM_2}{R^3} \sqrt{\frac{a}{GM_1}} R_x \left[\frac{3}{2} \frac{R_z}{R} \right] \left(\frac{a}{R} \right). \quad (44)$$

Finally, we integrate them along the trajectory of the passing star:

$$\begin{pmatrix} R_x \\ R_y \\ R_z \end{pmatrix} = \begin{pmatrix} R \cos(f_* + \omega_*) \\ R \sin(f_* + \omega_*) \cos i_* \\ R \sin(f_* + \omega_*) \sin i_* \end{pmatrix}, \quad (45)$$

where f_* is the true anomaly of the passing star. We integrate Eqs. (10) to (13) over time t from $-\infty$ to ∞ .

We integrate $\langle dh/dt \rangle$, $\langle dk/dt \rangle$, $\langle dp/dt \rangle$ and $\langle dq/dt \rangle$ by f_* instead of by t , using $df_*/dt = \sqrt{G(M_1 + M_2)(e_* + 1)D}/R^2$ and $R = (e_* + 1)D/(1 + e_* \cos f_*)$,

$$\begin{aligned} \Delta h &\simeq \int_{-\infty}^{\infty} \left\langle \frac{dh}{dt} \right\rangle dt = \int_{-\gamma}^{\gamma} \left\langle \frac{dh}{dt} \right\rangle \frac{R^2}{\sqrt{G(M_1 + M_2)(e_* + 1)D}} df_* \\ &= -\frac{15}{4(e_* + 1)^{5/2}} \frac{M_*}{\sqrt{M_* + 1}} \left(\frac{a}{D} \right)^{5/2} \cos \omega_* \left[\frac{1}{8} \gamma e_*^4 (5 \cos^2 i_* - 1) + f \right], \end{aligned} \quad (46)$$

$$\Delta k \simeq \frac{15}{4(e_* + 1)^{5/2}} \frac{M_*}{\sqrt{M_* + 1}} \left(\frac{a}{D} \right)^{5/2} \sin \omega_* \cos i_* \left[\frac{1}{8} \gamma e_*^4 (15 \cos^2 i_* - 11) + g \right], \quad (47)$$

$$\Delta p \simeq \frac{3}{8(e_* + 1)^{3/2}} \frac{M_*}{\sqrt{M_* + 1}} \left(\frac{a}{D}\right)^{3/2} (2\gamma + h) \sin 2i_*, \quad (48)$$

$$\Delta q \simeq \frac{e_*}{2} \left(\frac{1 - e_*^{-2}}{e_* + 1}\right)^{5/2} \frac{M_*}{\sqrt{M_* + 1}} \left(\frac{a}{D}\right)^{3/2} \sin i_* \sin 2\omega_*, \quad (49)$$

where γ is $\cos^{-1}(-1/e_*)$ and

$$f = \sqrt{e_*^2 - 1} \left[\frac{e_*^2}{6} (1 + 2e_*^2) - \frac{1}{24} (2 + e_*^2 + 12e_*^4) \sin^2 i_* + \frac{1}{6} (e_*^2 - 1)^2 \cos 2\omega_* \sin^2 i_* \right], \quad (50)$$

$$g = \sqrt{e_*^2 - 1} \left[\frac{e_*^2}{6} (1 + 2e_*^2) + \frac{1}{24} (2 - 19e_*^2 - 28e_*^4) \sin^2 i_* + \frac{1}{6} (e_*^2 - 1)^2 \cos 2\omega_* \sin^2 i_* \right], \quad (51)$$

$$h = \frac{2}{3} e_* \sqrt{1 - e_*^{-2}} \{ (e_*^{-2} - 1) \cos 2\omega_* + 3 \}. \quad (52)$$

Since we start with $h, k, p, q = 0$, the changes are equal to final h, k, p and q of the planetesimals. We obtain final e and i with $e = \sqrt{h^2 + k^2}$ and $i = \sqrt{p^2 + q^2}$. For $e_* = 1$, $f = g = h = \Delta q = 0$, e and i are

$$e \simeq \frac{15\pi}{128\sqrt{2}} \frac{M_*}{\sqrt{1 + M_*}} \left(\frac{a}{D}\right)^{5/2} \left[\cos^2 \omega_* \{5 \cos^2 i_* - 1\}^2 + \sin^2 \omega_* \cos^2 i_* \{15 \cos^2 i_* - 11\}^2 \right]^{1/2}, \quad (53)$$

$$i \simeq \frac{3\alpha}{8\sqrt{2}} \frac{M_*}{\sqrt{1 + M_*}} \left(\frac{a}{D}\right)^{3/2} \sin 2i_*. \quad (54)$$

ACKNOWLEDGMENTS

We thank Kiyoshi Nakazawa and Hiroyuki Emori for useful scientific discussions. We also thank John D. Larwood and Giovanni B. Valsecchi for critical comments, which helped us improve the original version of the manuscript, and Andeas Burkert for motivating us to study this problem. This work is supported in part by Grant-in-Aid for Specially Promoted Research of the Japanese Ministry of Education, Science, and Culture (11101002).

REFERENCES

- Adachi, I., Hayashi, C., and Nakazawa, K. 1976. The gas drag effect on the elliptical motion of a solid body in the primordial solar nebula. *Prog. Theor. Phys.* **56** 1756-1771.
- Adams, F. C., and G. Laughlin 2001. Constraints on the Birth Aggregate of the Solar System. *Icarus* **150** 151-162
- Andrillat, Y., M. Jaschek, and C. Jaschek 1990. The infrared spectrum of HD 141569. *Astron. Astrophys.* **233**, 474-476.

- Artymowicz, P. 1997. Beta Pictoris: an Early Solar System? *Annu. Rev. Earth Planet. Sci.* **25**, 175-219.
- Augereau, J. C., A. M. Lagrange, D. Mouillet, and F. Mnard 1999. ST/NICMOS2 observations of the HD 141569 A circumstellar disk. *Astron. Astrophys.* **350**, L51-L54.
- Backman, D. E., and F. Paresce 1993. Main-sequence stars with circumstellar solid material: the Vega phenomenon. In *Protostars and planets III* (E. H. Levy and J. Lunine, Eds.), pp. 1253-1304. Univ. of Arizona Press, Tucson. *Astrophys. J.* **450**, 1253-1304.
- Barnes, J. E., and L. Hernquist 1992. Dynamics of interacting galaxies. *Annu. Rev. Astron. Astrophys.* **30**, 705-742.
- Beckwith, S. V. W., and A. I. Sargent 1996. Circumstellar disks and the search for neighbouring planetary systems. *Nature* **383**, 139-144.
- Binney, J., and S. Tremaine 1987. *Galactic Dynamics*. Princeton Univ. Press, Princeton.
- Boffin, H. M. J., S. J. Watkins, A. S. Bhattal, N. Francis, and A. P. Whitworth, 1998. Numerical simulations of protostellar encounters - I. Star-disc encounters. *Mon. Not. R. Astron. Soc.* **300**, 1189-1204.
- Bodenheimer, P., and J. B. Pollack 1986. Calculations of the accretion and evolution of giant planets The effects of solid cores. *Icarus*, **67**, 391-408.
- Planetary dynamics in stellar clusters. *Mon. Not. R. Astron. Soc.* **322**, 859-865.
- Brouwer, D., and G. M. Clemence, 1961. *Methods of Celestial Mechanics*. Academic Press, New York.
- Brunini, A., and A. Fernández, 1996. Perturbations on an extended Kuiper disk caused by passing stars and giant molecular clouds. *Astron. Astrophys.* **308**, 988-994.
- Clarke, C. J., and J. E. Pringle 1991. Star-disc interactions and binary star formation. *Mon. Not. R. Astron. Soc.* **249**, 584-587.
- Clarke, C. J., and J. E. Pringle, 1993. Accretion disc response to a stellar fly-by. *Mon. Not. R. Astron. Soc.* **261**, 190-202.
- de la Fuente Marcos, C. and R. de la Fuente Marcos, 1997. Eccentric giant planets in open star clusters. *Astron. Astrophys.* **326**, L21-L24.
- Eggers, S., & M. M. Woolfson 1996. Stellar perturbations of inner core comets and the impulse approximation. *Mon. Not. R. Astron. Soc.* **282**, 13-18.
- Fajardo-Acosta, S. B., C. M. Telesco, C. M., and R. F. Knacke 1998. Infrared Photometry of beta Pictoris Type Systems. *Astron. J.* **115**, 2101-2121.

- Fernández, A. J. 1997, The Formation of the Oort Cloud and the Primitive Galactic Environment. *Icarus* **129**, 106-119.
- Goldreich, P., and S. Tremaine 1982. The dynamics of planetary rings. *Annu. Rev. Astron. Astrophys.* **20** 249-283.
- Goldreich, P., and W. R. Ward 1973. The Formation of Planetesimals. *Astrophys. J.* **183**, 1051-1062
- Greaves, J. S., and 10 colleagues, 1998. A Dust Ring around epsilon Eridani: Analog to the Young Solar System. *Astrophys. J.* **506**, L133-L137.
- Greenberg, R., W. K. Hartmann, C. R. Chapman, and J. F. Wacker, 1978. Planetesimals to planets - Numerical simulation of collisional evolution. *Icarus* **35**, 1-26.
- Hall, S. M. 1997. Circumstellar disc density profiles: a dynamic approach. *Mon. Not. R. Astron. Soc.* **287**, 148-154.
- Hall, S. M., C. J. Clarke, and J. E. Pringle 1996. Energetics of star-disc encounters in the non-linear regime. *Mon. Not. R. Astron. Soc.* **278**, 303-320.
- Hayashi, C. 1981. Structure of the solar nebula, growth and decay of magnetic fields and effects of magnetic and turbulent viscosities on the nebula. *Prog. Theor. Phys. Suppl.* **70**, 35-53.
- Hayashi, C., K. Nakazawa, and Y. Nakagawa 1985. Formation of the solar system. In *Protostars and Planets II* (D. C. Black and M. S. Matthews, Eds.), pp. 1100-1153. Univ. of Arizona Press, Tucson.
- Heggie, D. C., and F. A. Rasio 1996. The Effect of Encounters on the Eccentricity of Binaries in Clusters. *Mon. Not. R. Astron. Soc.*, **282**, 1064-1084.
- Heller, C. H. 1993. Encounters with protostellar disks. I - Disk tilt and the nonzero solar obliquity. *Astrophys. J.* **408**, 337-346.
- Heller, C. H. 1995. Encounters with Protostellar Disks. II. Disruption and Binary Formation. *Astrophys. J.* **455**, 252-259
- Heppenheimer, T. A. 1978. On the formation of planets in binary star systems. *Astron. Astrophys.* **65**, 421-426.
- Ida, S., J. Larwood, and A. Burkert 2000. Evidence for Early Stellar Encounters in the Orbital Distribution of Edgeworth-Kuiper Belt Objects. *Astrophys. J.* **528**, 351-356.
- Ikoma, M., K. Nakazawa, and H. Emori 2000. Formation of Giant Planets: Dependences on Core Accretion Rate and Grain Opacity. *Astrophys. J.* **537**, 1013-1025.
- Ito, T., and Tanikawa, K. 2001. Stability of Terrestrial Protoplanet Systems and Alignment of Orbital Elements. *PASJ* **53**, 143-151.

- Jayawardhana, R., S. Fisher, L. Hartmann, C. Telesco, R. Pina, and G. Fazio 1998. A Dust Disk Surrounding the Young A Star HR 4796A. *Astrophys. J.* **503**, L79-L82.
- Jura, M., A. M. Ghez, R. J. White, D. W. McCarthy, R. C. Smith, and P. G. Martin 1995. The fate of the solid matter orbiting HR 4796A. *Astrophys. J.* **455**, 451-456.
- Jourdain de Muizon, M., and 10 colleagues, 1999. A very cold disc of dust around the G0V star HD 207129. *Astron. Astrophys.* **350**, 875-882.
- Kalas, P., J. Larwood, B. A. Smith, and A. Schultz 2000. Rings in the Planetesimal Disk of β Pictoris. *Astrophys. J.* **530**, 133-137.
- Kalas, P., and D. Jewitt 1995. Asymmetries in the Beta Pictoris Dust Disk *Astron. J.* **110**, 794-804.
- Korycansky, D. G., and J. C. B. Papaloizou 1995. The response of a gaseous disc to a binary encounter *Mon. Not. R. Astron. Soc.* **274**, 85-98.
- Kroupa, P. 1995. The dynamical properties of stellar systems in the Galactic disc. *Mon. Not. R. Astron. Soc.* **277** 1507-1521.
- Kroupa, P. 1998. On the binary properties and the spatial and kinematical distribution of young stars. *Mon. Not. R. Astron. Soc.* **298**, 231-242.
- Larwood, J. D., and P. G. Kalas 2001. Close stellar encounters with planetesimal disks: The dynamics of asymmetry in the β Pictoris system. *Mon. Not. R. Astron. Soc.* **323**, 402-416.
- Larwood, J. D. 1997. The tidal disruption of protoplanetary accretion discs. *Mon. Not. R. Astron. Soc.* **290**, 490-504.
- Laughlin G., and F. C. Adams 1998. The Modification of Planetary Orbits in Dense Open Clusters. *Astrophys. J.* **508**, L171-L174.
- Laughlin G., and F. C. Adams 2000. The frozen Earth: Binary scattering events and the fate of the Solar. *Icarus*, **145**, 614-627.
- Lissauer, J. J., and G. R. Stewart, 1993. Growth of planets from planetesimals. In *Protostars and planets III* (E. H. Levy and J. Lunine, Eds.), pp. 1061-1088. Univ. of Arizona Press, Tucson.
- Marzari, F., and H. Scholl 2000. Planetesimal Accretion in Binary Star Systems. *Astrophys. J.*, **543**, 328-339.
- Mizuno, H. 1980. Formation of the Giant Planets. *Prog. Theor. Phys.*, **64**, 544-557.
- Ohtsuki, K., S. Ida, Y. Nakagawa, and K. Nakazawa 1993. Planetary accretion in the solar gravitational field. In *Protostars and Planets III* (E. H. Levy & J. Lunine Eds.), pp. 1089-1107. Univ. Arizona Press, Tucson.

- Ohtsuki, K. 1993. Capture probability of colliding planetesimals - Dynamical constraints on accretion of planets, satellites, and ring particles. *Icarus* **106**, 228-246.
- Ostriker, E. C. 1994. Capture and induced disk accretion in young star encounters. *Astrophys. J.* **424**, 292-318.
- Palmer, P. L. & J. Papaloizou, 1982. Tidal interactions of disc galaxies. *Mon. Not. R. Astron. Soc.* **199**, 869-882.
- Safronov, V. S. 1969. *Evolution of the Protoplanetary Cloud and Formation of the Earth and Planets*. Nauka Press, Moscow.
- Sahu, M. S., J. C. Blades, L. He, D. Hartmann, M. J. Barlow, and I. A. Crawford 1998. Atomic and Molecular Interstellar Absorption Lines toward the High Galactic Latitude Stars HD 141569 and HD 157841 at Ultra-High Resolution. *Astrophys. J.* **504**, 522-532.
- Stern, S. A. 1995. Collisional time scales in the Kuiper disk and their implications. *Astrophys. J.* **110**, 856-868.
- Toomre, A., and J. Toomre 1972. Galactic Bridges and Tails. *Astrophys. J.* **178**, 623-666.
- Wahde, M., K. J. Donner, and B. Sundelius 1996. Dynamical friction in disc galaxies with non-zero velocity dispersion. *Mon. Not. R. Astron. Soc.* **281**, 1165-1182.
- Weidenschilling, S. J., and J. N. Cuzzi 1993. Formation of planetesimals in the solar nebula. In *Protostars and Planets III* (E. H. Levy and J. I. Lunine Eds.), pp. 1031-1060. Univ. of Arizona Press, Tucson.
- Weinberger, A. J., E. E. Becklin, G. Schneider, B. A. Smith, P. J. Lowrance, M. D. Silverstone, B. Zuckerman, and R. J. Terri 1999. The Circumstellar Disk of HD 141569 Imaged with NICMOS. *Astrophys. J.* **525**, L53-L56.
- Weinberger, A. J., R. M. Rich, E. E. Becklin, B. Zuckerman, and K. Matthews 2000. Stellar Companions and the Age of HD 141569 and Its Circumstellar Disk. *Astrophys. J.* **544**, 937-943.
- Wetherill, G. W. 1980. Formation of the terrestrial planets. *Annu. Rev. Astron. Astrophys.* **18**, 77-113.
- Whitmire, D. P., J. J. Matese, L. Criswell, and S. Mikkola 1998. Habitable Planet Formation in Binary Star Systems. *Icarus*, **132**, 196-203.
- Yabushita, S., I. Hasegawa, and K. Kobayashi 1982. The stellar perturbations of orbital elements of long-period comets. *Mon. Not. R. Astron. Soc.* **200**, 661-671.

Fig. 1.— Encounter configuration in the frame centered at the primary star with mass M_1 . The orbit of the passing star with mass M_2 is characterized by pericenter distance D , eccentricity e_* , inclination i_* and argument of perihelion ω_* . If length and mass are scaled by D and M_1 , the encounter parameter are M_* ($= M_2/M_1$), e_* , i_* and ω_* .

Fig. 2.— Left and center panels are the time evolution of orbital eccentricity e and inclination i of particles as a function of scaled initial semimajor axis a/D . Time proceeds from (a) top to (c) bottom panels. The right panels are face-on snapshots of the disk particles (small dots) and the passing star (filled circle).

Fig. 3.— (a) Orbital eccentricity e and inclination i of particles pumped-up by a passing star, as a function of initial scaled semimajor axis a/D , in the case with $i_* = 5^\circ$, $\omega_* = 90^\circ$, $e_* = 1$ and $M_* = 1$. (b) The results with $e_* = 1$ and $M_* = 0.2$ (i_* and ω_* are the same). (c) The result with $e_* = 5$ and $M_* = 1$. Dashed lines with triangles express analytical expression given by Eqs. (46) to (49) in Appendix. The dashed lines (in particular, for i) are almost indistinguishable from the numerical results in the inner region.

Fig. 4.— Orbital eccentricity e and inclination i of particles pumped-up by a passing star, as a function of scaled semimajor axis a/D , in the case with $\omega_* = 0^\circ$, $e_* = 1$ and $M_* = 1$. Orbital inclination of the passing star is (a) 5° , (b) 30° , (c) 45° , (d) 85° and (e) 150° . Dashed lines with triangle express analytical expression given by Eqs. (15) and (16) in Section 5. The dashed lines are almost distinguishable from the numerical results.

Fig. 5.— Numerically and analytically calculated \tilde{e}_0 are plotted, \tilde{e}_0 is defined by $e = (15\pi/64)\tilde{e}_0 (a/D)^{5/2}$ in the inner disk, in the case with $e_* = 1$ and $M_* = 1$. (a) The contours of \tilde{e}_0 numerically calculated at every 10 degrees of i_* and ω_* . (b) The contours of analytically calculated \tilde{e}_0 : $[\cos^2 \omega_* \{1 - (5/4) \sin^2 i_*\}^2 + \sin^2 \omega_* \cos^2 i_* \{1 - (15/4) \sin^2 i_*\}^2]^{1/2}$ (Eq. (15)), as a function of i_* and ω_* .

Fig. 6.— Numerically and analytically calculated \tilde{i}_0 are plotted, where \tilde{i}_0 is defined by $i = 3\pi/16\tilde{i}_0 (a/D)^{3/2}$ in the inner disk, in the case with $e_* = 1$ and $M_* = 1$. Circles are numerical results. We calculated the case with ω_* at every 10° from 0° to 90° , for each i_* . The results overlap each other: \tilde{i}_0 is almost completely independent of ω_* . Dashed lines express analytical expression of \tilde{i}_0 : $\sin 2i_*$ (see Eq. (16)).

Fig. 7.— The relative change in semimajor axis Δa after a stellar encounter as a function of initial semimajor axis a in the case with $i_* = 5^\circ$, $\omega_* = 90^\circ$, $M_* = 1$ and $e_* = 1$.

Fig. 8.— (a) orbital eccentricity e , (b) inclination i , (c) longitude of pericentre $\tilde{\omega}$ and (d) longitude of ascending node φ of planetesimals, as a function of initial semimajor axis a/D , in the case with initial e and i , $i_* = 5^\circ$, $\omega_* = 0^\circ$, $e_* = 1$ and $M_* = 1$.

Fig. 9.— (a) e_{eff} and i_{eff} , (b) e_{rel} and i_{rel} and (c) e and i , of the colliding planetesimals, as a function of initial semimajor axis a/D , where we define a is the radius of the colliding point. $(e_0, i_0) = (0, 0)$ and $(i_*, \omega_*, M_*, e_*) = (5^\circ, 0^\circ, 1, 1)$.

Fig. 10.— The same as Fig. 8 except for e_0 and i_0 are 1×10^{-4} .

Fig. 11.— The same as Fig. 9 except for e_0 and i_0 are 1×10^{-4} .

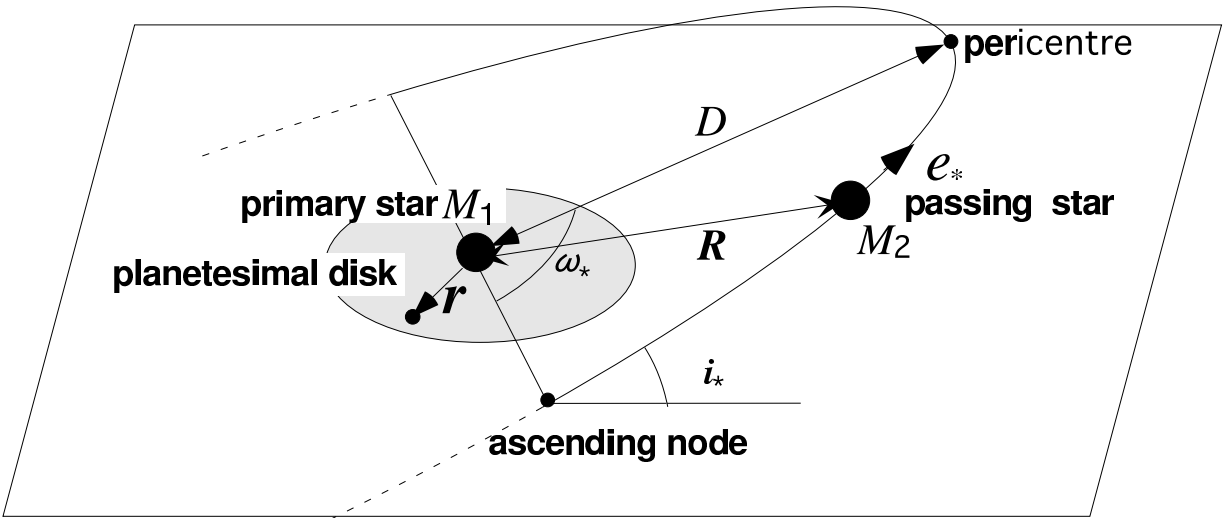


Fig. 1 — Kobayashi and Ida (2001)

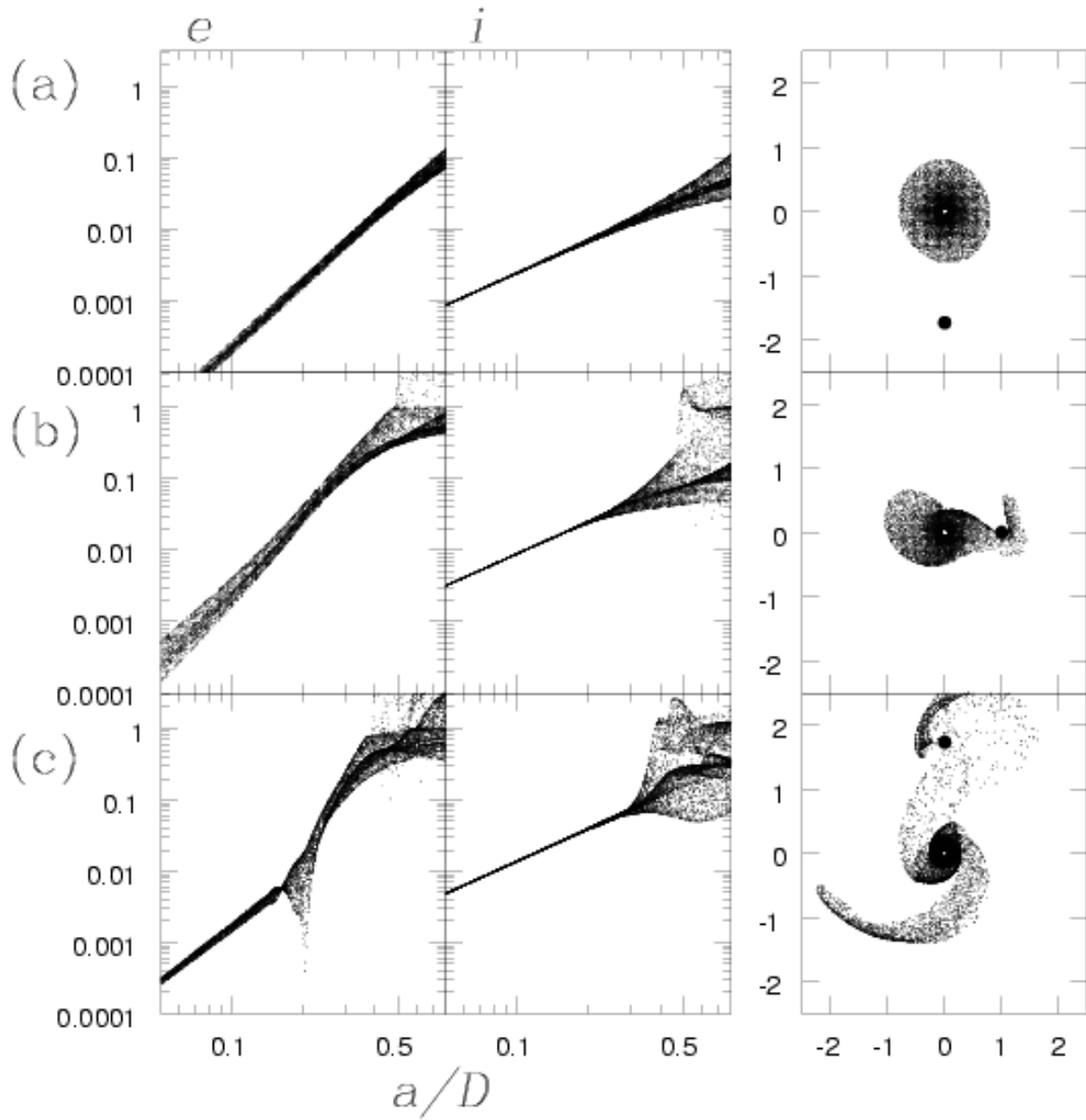


Fig. 2 — Kobayashi and Ida (2001)

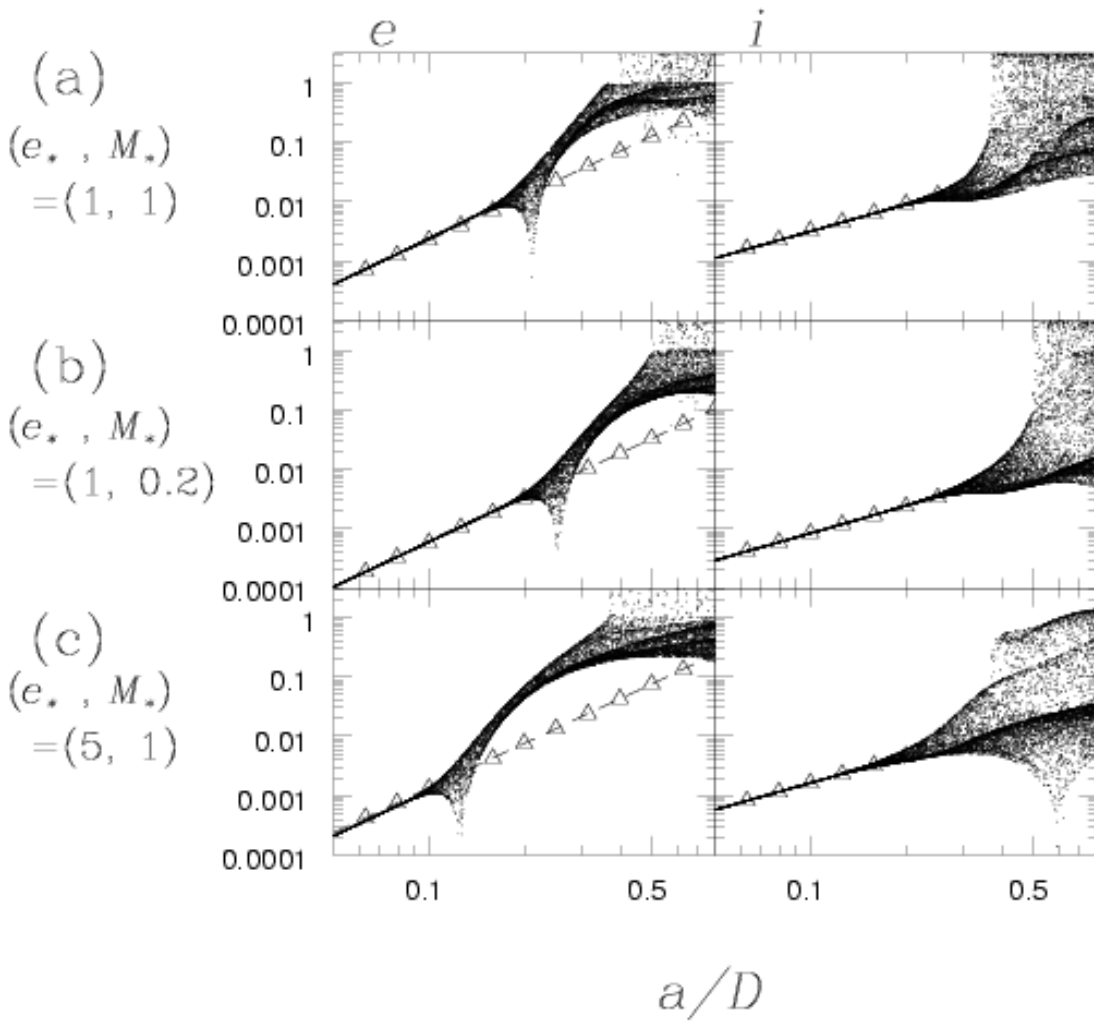


Fig. 3 — Kobayashi and Ida (2001)

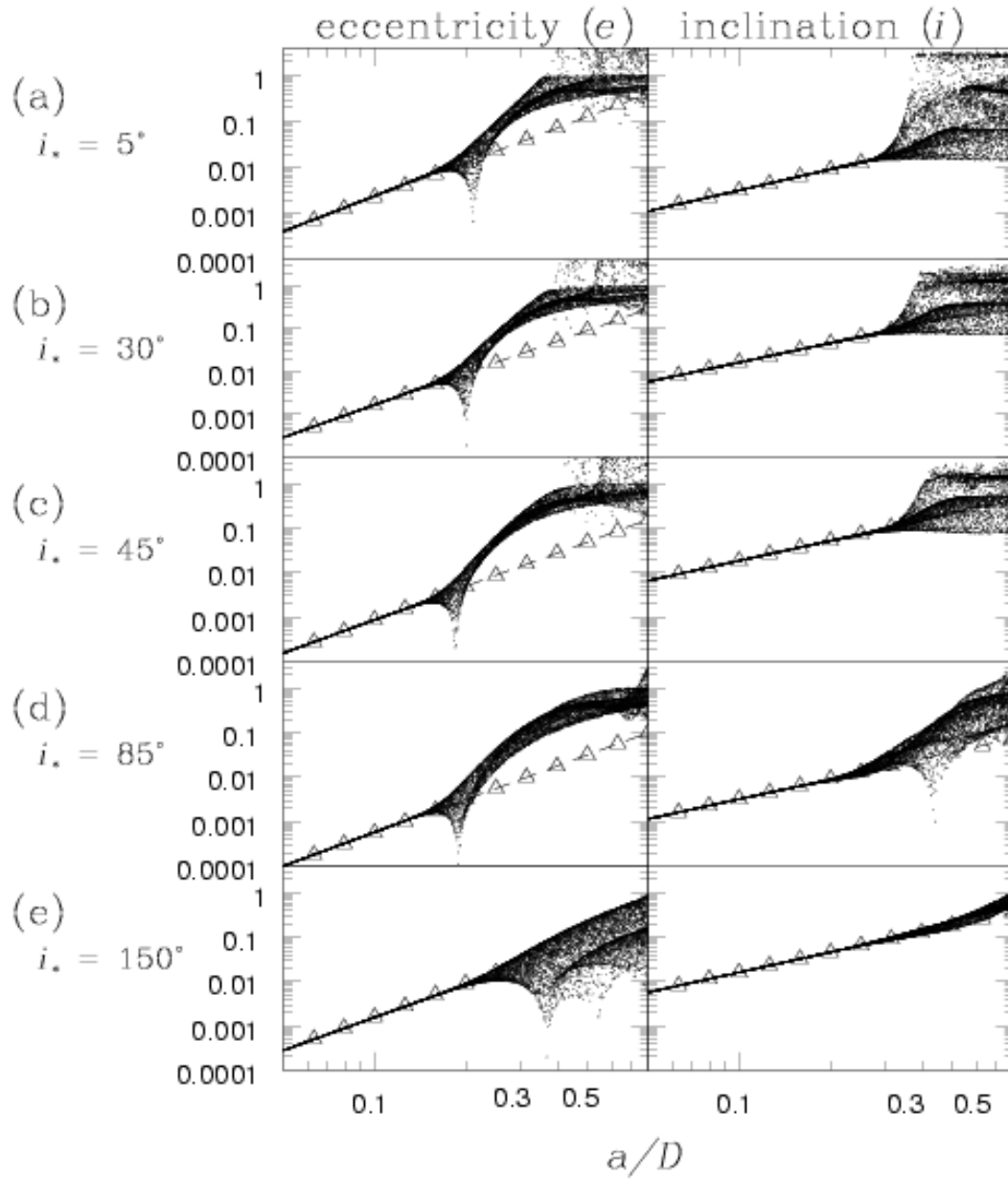


Fig. 4 — Kobayashi and Ida (2001)

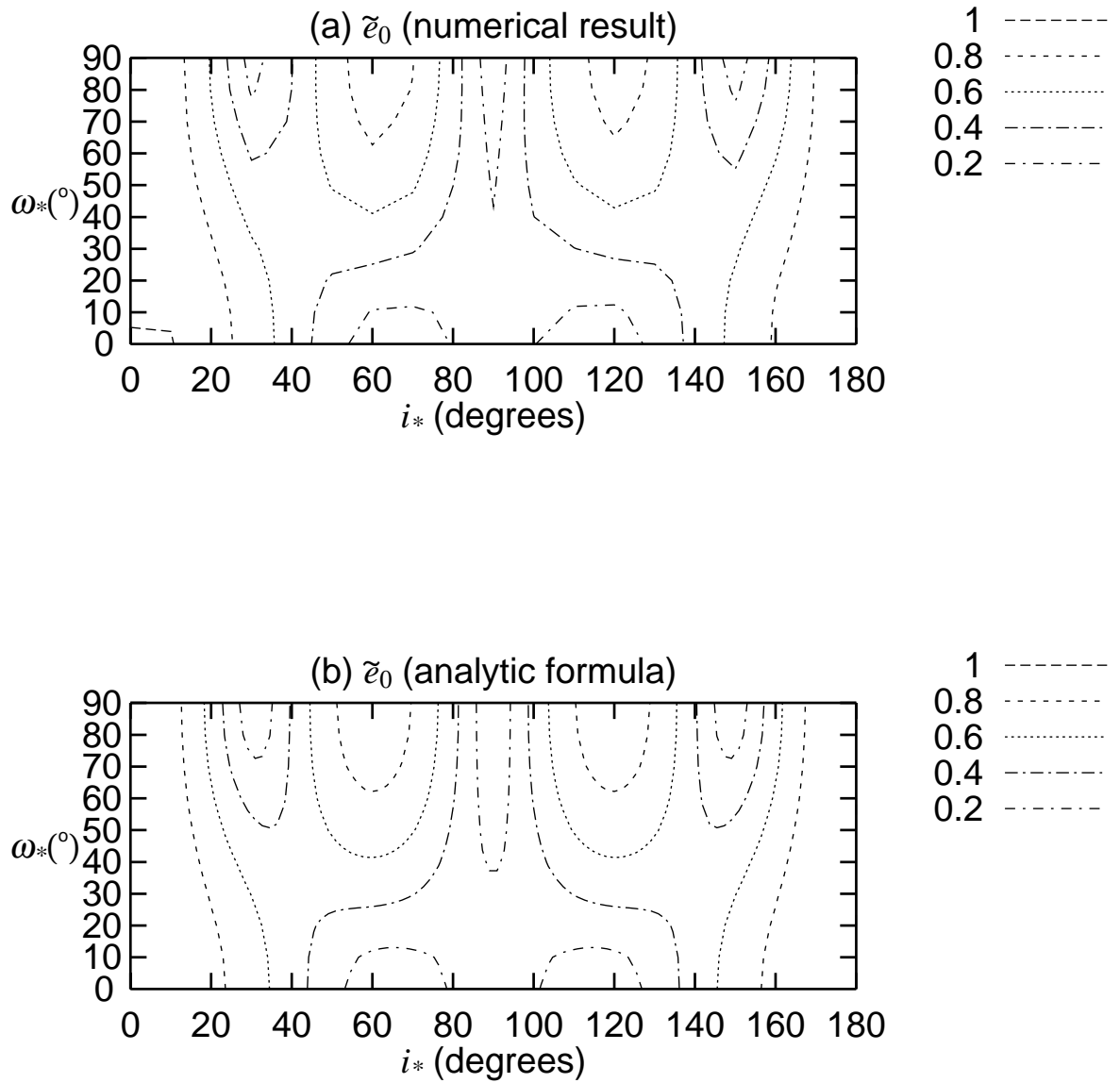


Fig. 5 — Kobayashi and Ida (2001)

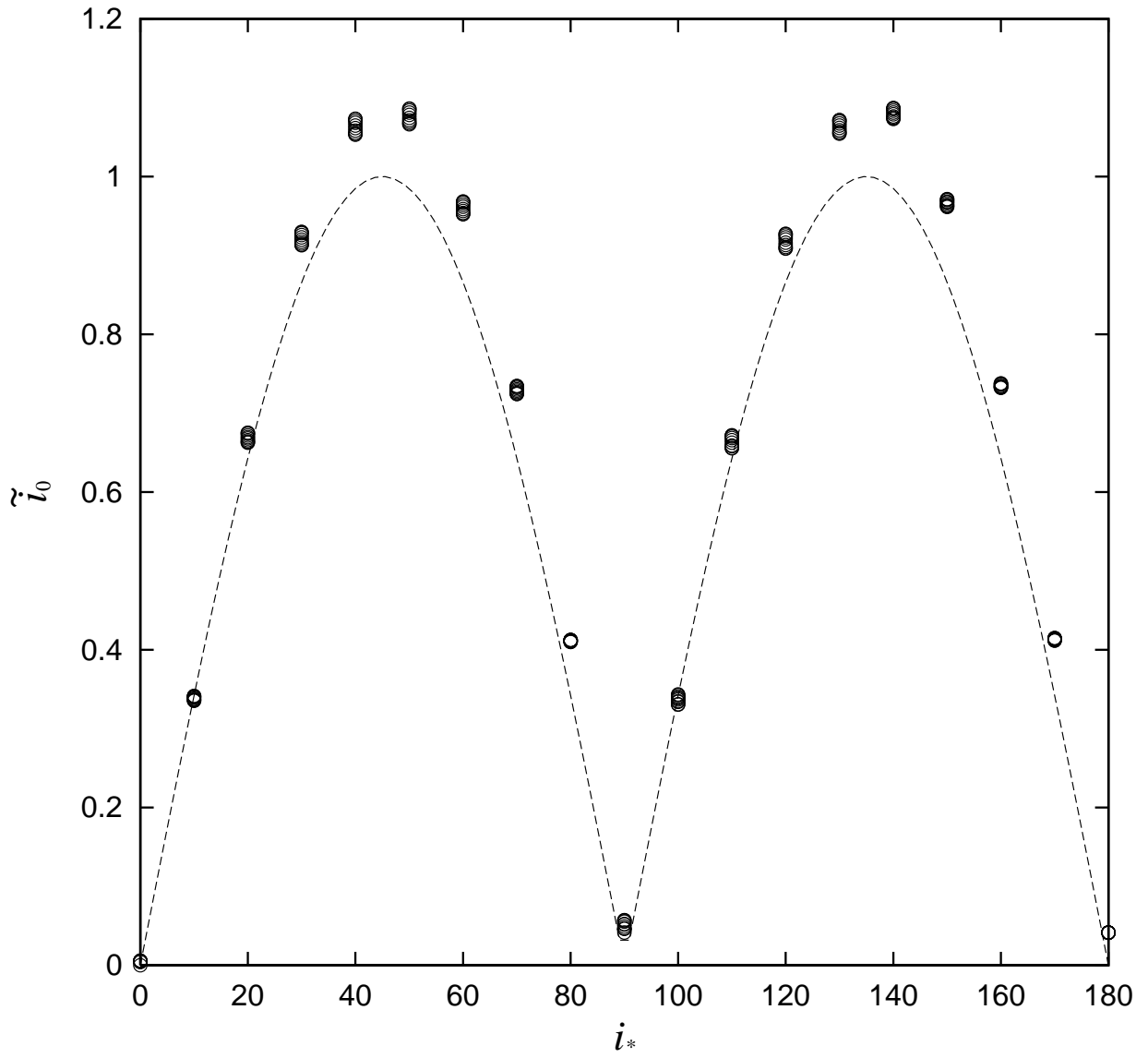


Fig. 6 — Kobayashi and Ida (2001)

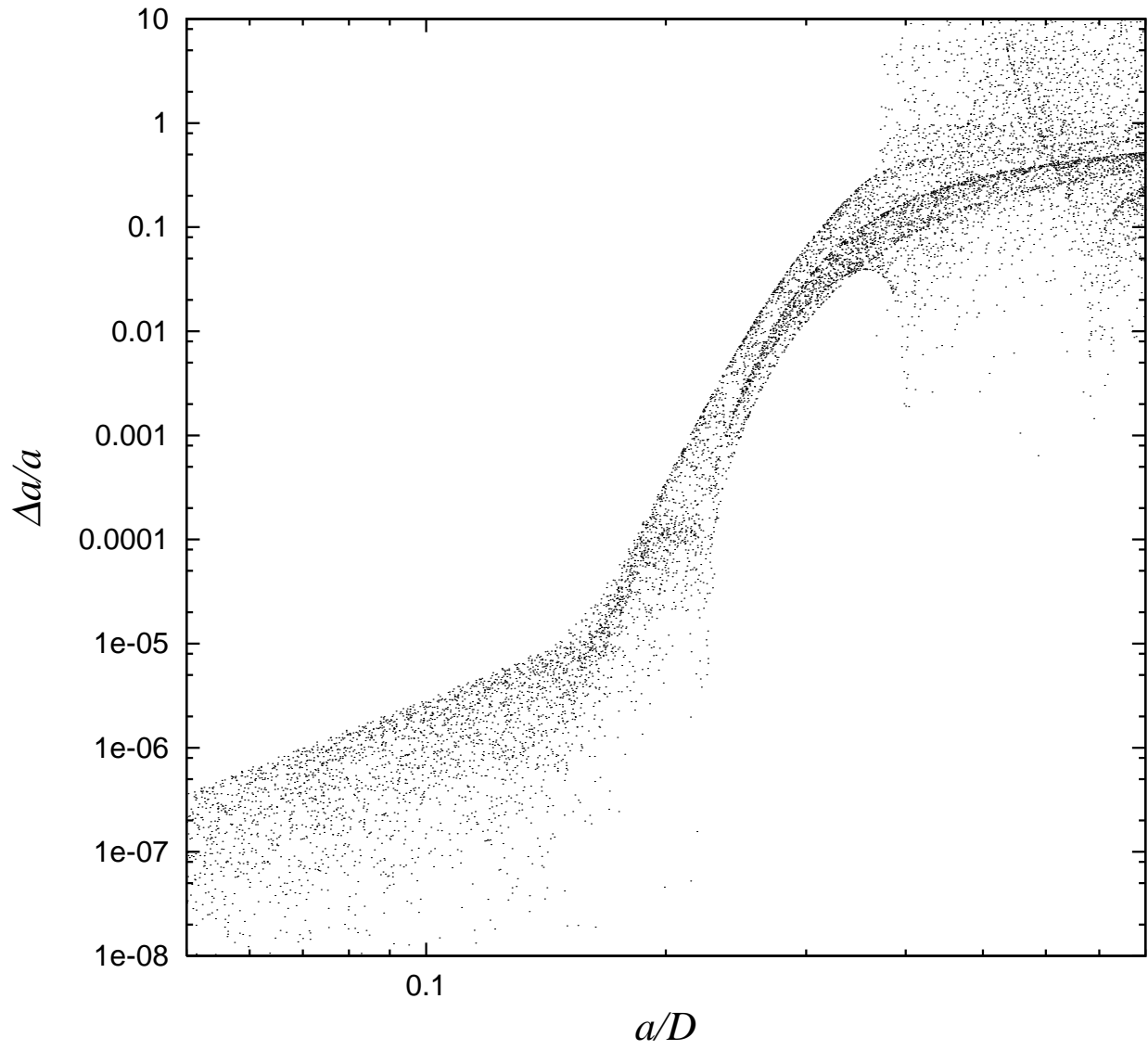


Fig. 7 — Kobayashi and Ida (2001)

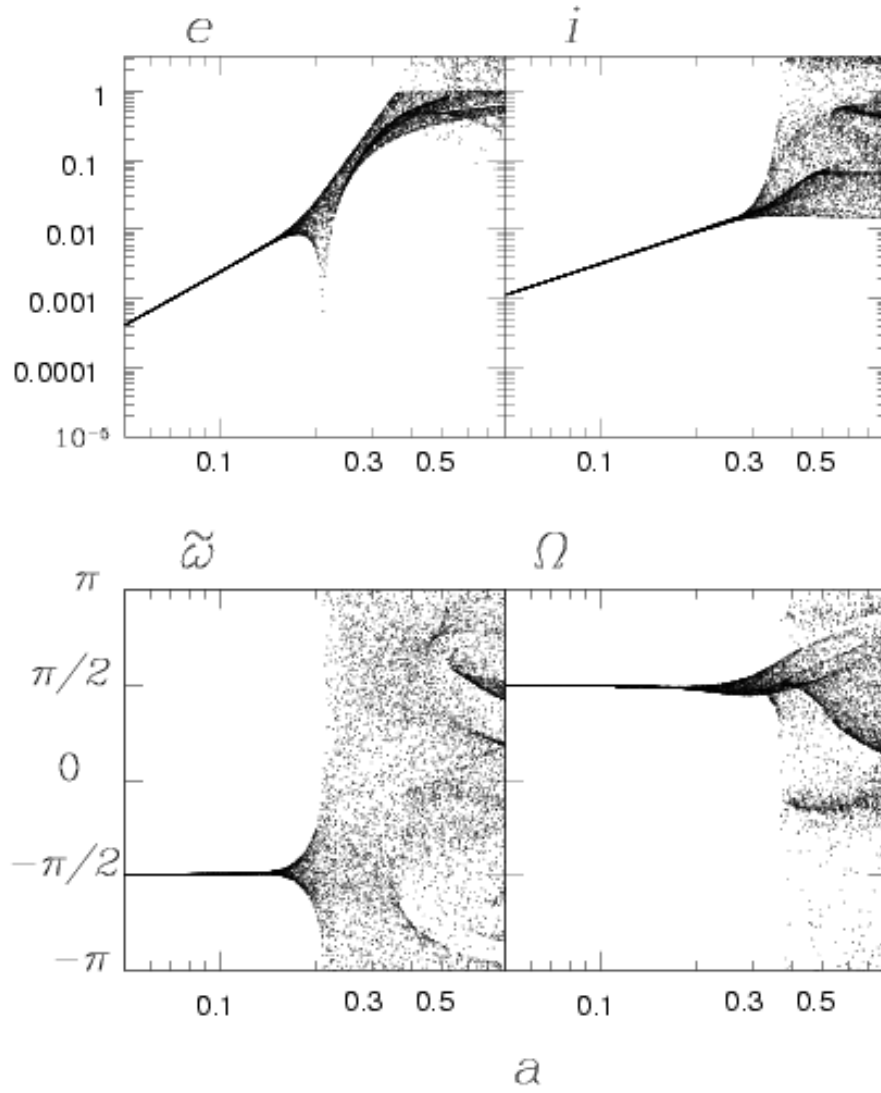


Fig. 8 — Kobayashi and Ida (2001)

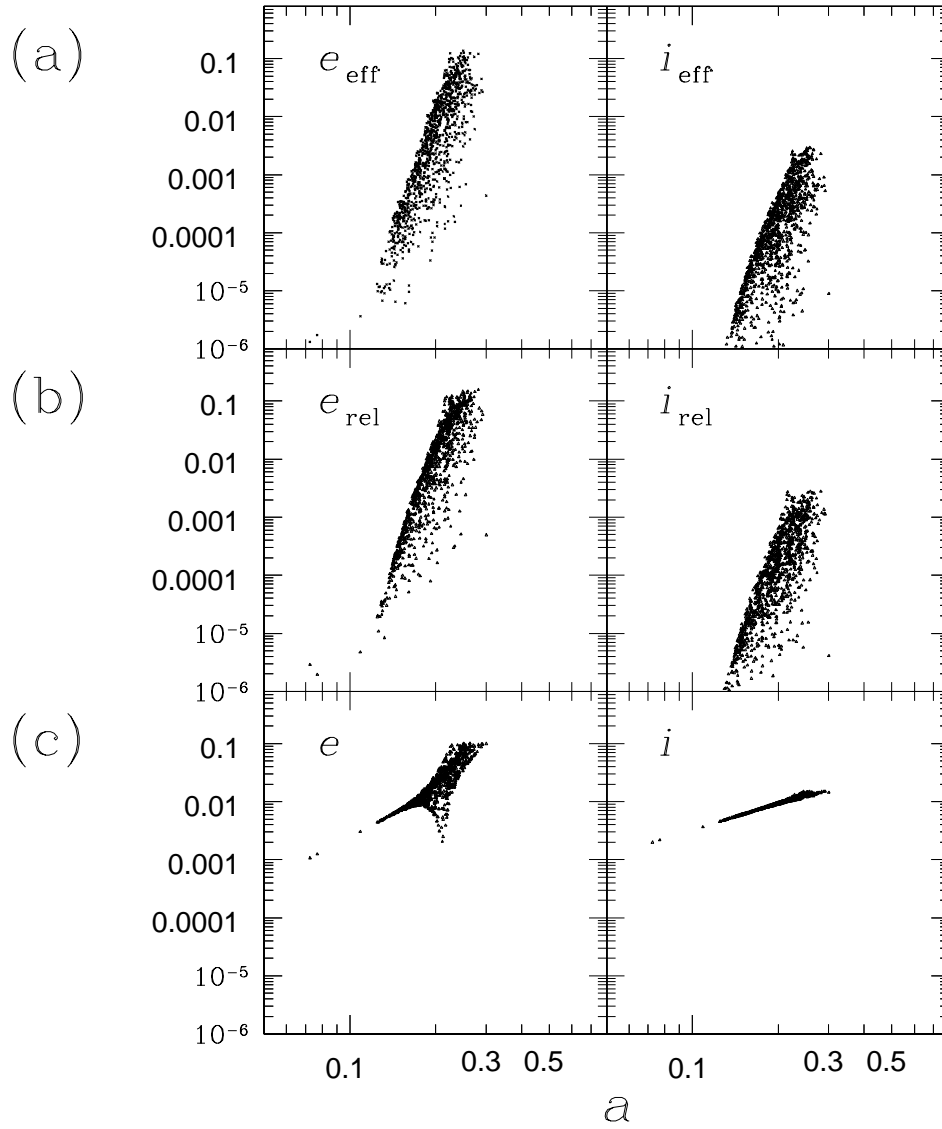


Fig. 9 — Kobayashi and Ida (2001)

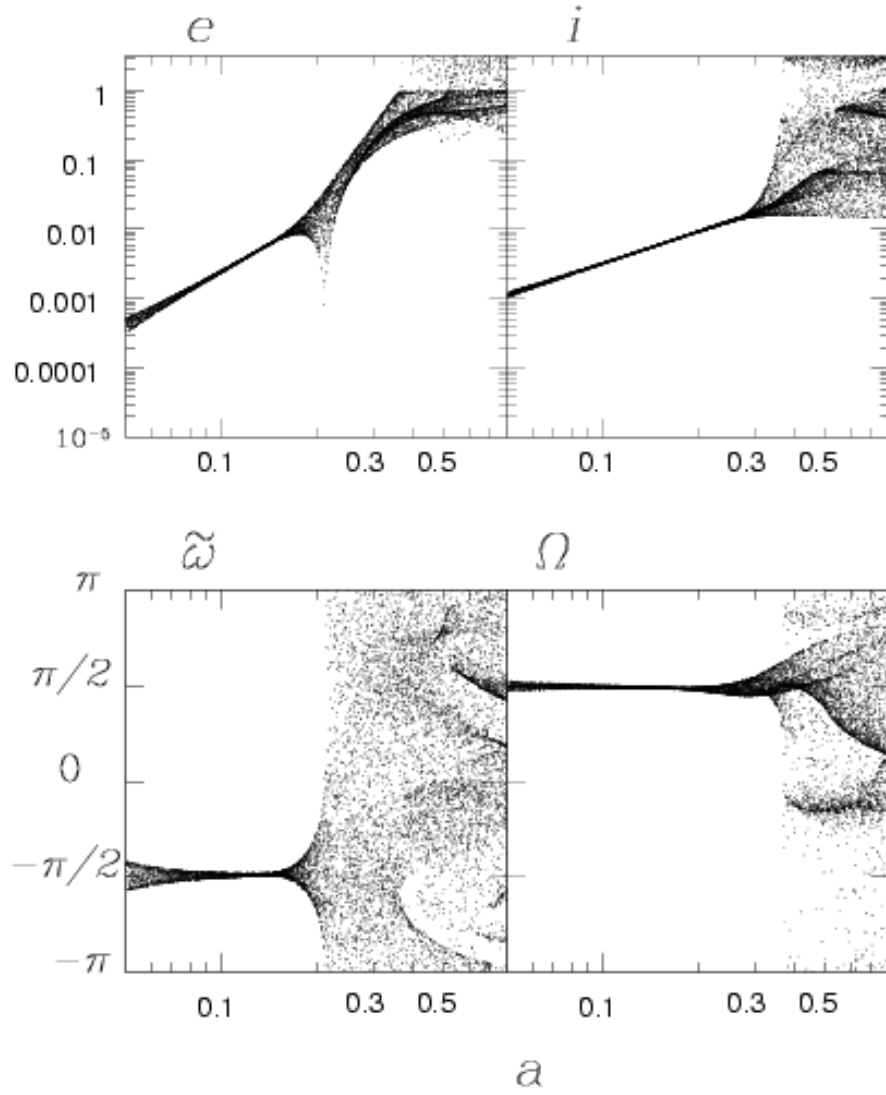


Fig. 10 — Kobayashi and Ida (2001)

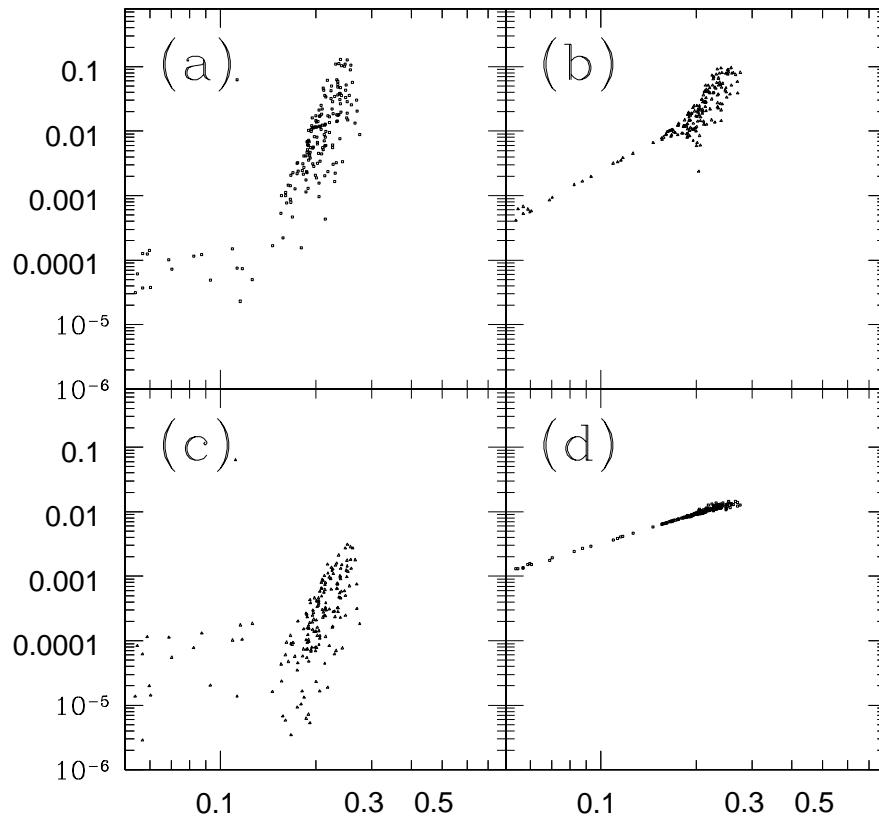


Fig. 11 — Kobayashi and Ida (2001)